Norwegian University of Life Sciences

Master's Thesis 2023 30 ECTS
Faculty of Science and Technology

Climate responses to a rapid phaseout of Black Carbon emissions, with a focus on the Asian summer monsoon

Julia Helena Navdahl
Environmental Physics and Renewable Energy

ABSTRACT

The absorption of shortwave radiation by aerosols is predominantly caused by black carbon (BC), which can significantly affect atmospheric stability, circulation, and the hydrological cycle. Driven by concerns over air quality, public health, and global warming, a reduction in BC emissions is anticipated in the coming decades. This shift is of particular significance in South and East Asia, regions identified as aerosol hotspots, where large populations and the reliance on the Asian summer monsoon (ASM) make them especially susceptible to changes in aerosol dynamics.

This thesis comprehensively analyzes the climatic responses to a global phaseout in BC emissions under the SSP3-7.0 scenario. Utilizing simulations from three distinct climate models within the Coupled Model Intercomparison Project Phase 6 (CMIP6) experiment—UKESM1.0-LL, MIROC6, and MPI-ESM1.2-HAM—this study spans the period from 2015 to 2054 (and to 2094 for UKESM1.0-LL) to project global, regional, and seasonal anomalies. The focus is on examining the responses in Aerosol Absorption Optical Depth (AAOD), near-surface temperature, vertical mass flux, vertical air temperature, precipitation, and their interdependencies across each model.

The results reveal significant inter-model differences. MIROC and MPI-ESM exhibit weaker responses to BC emission reductions, aligning closely with the ASM's typical behavior. In contrast, UKESM projects a robust decrease in precipitation over India, counter to expectations, attributed to reduced convective activity. This variance in responses emphasizes the challenges in climate modeling, mainly due to the poorly constrained nature of aerosol absorption and the complex mechanisms driving the Asian climate system. The thesis provides insights into the potential impact of climate policies aimed at mitigating BC emissions.

ACKNOWLEDGMENTS

First, I would like to express my sincere gratitude to my supervisor, Professor Bjørn H. Samset, for his invaluable guidance and enthusiasm throughout the process of working on this thesis. He provided me with insights into the complex field of aerosol research and took time out of his busy schedule to give constructive feedback and encouragement, which I genuinely appreciate.

I would also like to thank Marit Sandstad for assisting with the coding for the simulations and Laura Wilcox for helping with interpreting the results. Their contributions were instrumental in completing this thesis.

I want to thank my brother, Sebastian, for supporting me throughout this process. He showed a keen interest in my project and provided pictures from his recent trip to India, as well as taking the time to review my thesis, which I genuinely appreciate.

Looking back on my time at NMBU, I must say that it has been an extraordinary five and a half years spent in the "Ås-bubble." It has truly been rewarding for me, as it allowed me to grow academically and develop valuable friendships that will last a lifetime. I want to extend a special thanks to my amazing classmates and friends for making this chapter of my life fun, enlightening, transformative, and full of unforgettable memories.

Lastly, my deepest appreciation goes to my dear parents, Jolanta and Johnny, and my brothers, Sebastian, Alexander, and Kristian, for their unconditional support.

CONTENTS

List of Figures and Tables

ACRONYMS

AAOD Aerosol Absorption Optical Depth

ACI Aerosol-Cloud Interaction

AerChemMIP Aerosol and Chemistry Model Intercomparison Project

AERONET Aerosol Robotic Network

AOD Aerosol Optical Depth

ARI Aerosol-Radiation Interaction

ASM Asian Summer Monsoon

BC Black Carbon

BrC Brown Carbon

CLE Current Legislation Emission

CMIP6 Coupled Model Intercomparison Project Phase 6

CNN Cloud Condensation Nuclei

ERF Effective Radiative Forcing

ESM Earth System Model

fSST fixed Sea-Surface Temperatures

GCM Global Climate Model

GHG Greenhouse Gas

ITCZ Intertropical Convergence Zone

INPs Ice-Nucleating Particles

IPCC Intergovernmental Panel on Climate Change

MAC Mass Absorption Cross-section

MTFR Maximum Technically Feasible Reduction

NTCF Near-Term Climate Forcer

RCP Representative Concentration Pathway

RF Radiative Forcing

SLCF Short-Lived Climate Forcer

SSA Single-Scattering Albedo

SSP Shared Socio-economic Pathway

TOA Top of Atmosphere

WMGHG Well-Mixed Greenhouse Gases

1 Introduction

This section provides necessary background information to emphasize the importance of studying climate response to mitigations in black carbon emissions.

1.1 Background

According to the Sixth Assessment Report (AR6) presented by the Intergovernmental Panel on Climate Change (IPCC), it is an undeniable fact that human actions have caused global warming of about 1.1°C since the pre-industrial era (IPCC, 2021). This is primarily due to greenhouse gas (GHG) emissions caused by energy consumption, land use, and lifestyles. To achieve the goal of limiting global warming to 1.5°C, substantial measures to reduce the emission of GHGs are needed (Millar et al., 2017). This action may also significantly reduce emissions of anthropogenic aerosols, which are often co-emitted with GHGs (Samset, B. et al., 2018).

Aerosols are tiny particles suspended in the atmosphere. They have an essential role in the global and regional climate system, as they can warm and cool the atmosphere depending on their composition and optical properties (Shindell et al., 2008). On a global scale, it is estimated that aerosol emissions have counteracted almost one-third of the global warming due to GHGs (IPCC, 2013; Ramachandran et al., 2022).

With the onset of industrialization in the 1850s, aerosol emissions surged globally. In response to evidence of the adverse effects of air pollution on public health and the environment, western governments took measures to reduce emissions in the late 1970s and 1980s (Fowler et al., 2020; Rao, Shilpa et al., 2017). Meanwhile, South and East Asian economies emerged as significant sources of aerosol emissions, driven by rapid economic growth and expanding populations (Lund et al., 2023; Mosley, 2014). India and China have become the largest source of anthropogenic aerosols and their precursors in the last few decades (Li, Z. et al., 2016). While China has recently made significant advances in reducing emissions, India's emissions continue to increase, creating a so-called dipole emission pattern (Li, C. et al., 2017; Ramachandran et al., 2022).

Anthropogenic aerosols have been causing changes in climate patterns across South and East Asia for an extended period. Their influence may surpass that of the steadily rising concentrations of GHGs, particularly in affecting precipitation (Lau, W. K. M., 2016; Samset et al., 2019). The apparent sensitivity of anthropogenic aerosols to the hydrological cycle is twice that of GHGs (Kloster et al., 2010; Salzmann, 2016; Samset et al., 2016), and the response of global mean precipitation to aerosol perturbations can have a more rapid effect on shortwave transmissivity and, thus, a substantial influence on radiative energy imbalance (Andrews et al., 2010; Liepert & Previdi, 2009; Liu, L. et al., 2018).

Figure 1.1: Air pollution over the India Gate in central New Delhi, October 2023 (photograph by Sebastian Navdahl).

Sulfate aerosols can scatter shortwave radiation, ultimately contributing to cooling the Earth's surface. In contrast, black carbon (BC) aerosols are known for absorbing both solar and terrestrial radiation, leading to localized atmospheric heating while initially cooling the surface (Ramanathan & Carmichael, 2008). Driven by concerns over air quality, public health, and global warming, significant and rapid changes in aerosol emissions are expected in the

coming decades. The effects of these changes on regional and global climate and weather patterns are uncertain, especially regarding the role of BC. Since South and East Asia alone contribute to approximately 45% of global anthropogenic BC emissions (Klimont et al., 2017), conducting a thorough study of this region is crucial.

1.2 Motivation and Objective

The dipole emission patterns of aerosols in Asia alter the aerosol-radiation-cloud radiative forcing (RF), potentially triggering atmospheric reactions and regional anomalies. These shifts can have consequences extending beyond the Asian aerosol source region, affecting climate, chemical reactions, and cloud formation (Ramachandran et al., 2022; Samset et al., 2019). The South and East Asian regions are particularly vulnerable to future changes due to their dependence on the Asian summer monsoon (ASM), which may also be modified. This weather phenomenon holds significant socioeconomic importance for the region, particularly India and China, representing over one-third of the world's population (Li, Z. et al., 2016).

BC emissions, which are responsible for roughly 60% of the overall aerosol absorption in current global climate models (Sand, M. et al., 2021), are projected to decrease rapidly in India and China in the following decades as they are a target for emission control (Rönkkö et al., 2023; Streets et al., 2013). Regulating these particles to protect human health and climate may have unintended consequences for the climate, such as altered surface temperature and precipitation rates, as demonstrated by previous studies (e.g., Acosta Navarro et al. (2017); Bond et al. (2013); Rotstayn et al. (2013); Wilcox et al. (2020)). On a global scale, the expected climate impacts from mitigating aerosol burden are projected to be insignificant, considering the increasing dominance of RF from GHGs (Samset, 2016). However, at a regional level, these reductions may yield noteworthy ramifications.

In this thesis, we examine the implications of BC emissions on climate, delving into the complexities and uncertainties involved in mitigating them. Model projections of the influence of BC emissions on climate include numerous spatial and temporal uncertainties (Samset, B. H. et al., 2018; Wilcox et al., 2020). The climate dynamics of South and East Asia, regions particularly vulnerable to climate change (Samset et al., 2019), are shaped by a complex interplay of atmospheric, oceanic, and terrestrial processes (Li, J. et al., 2022; Zelinka

et al., 2020). This complexity is further compounded by the Asian monsoon season, leading to varied projections across different climate models.

This thesis aims to assess the impact of phasing out BC emissions on key climate variables - namely aerosol absorption optical depth, near-surface temperature, precipitation, vertical temperature, and vertical mass flux - utilizing three distinct CMIP6 global climate models: UKESM1.0-LL, MIROC6, and MPI-ESM1.2-HAM. The models are analyzed under a modification of the future scenario SSP3-7.0, where global BC emissions are rapidly reduced, considering global, regional, and seasonal implications. The focus is mainly on India and China, regions where the repercussions of such changes are most critical. This research seeks to elucidate the potential enhancement of changes in these climate variables and draws contrasts between the outcomes from different models. By examining the effects of BC emission mitigation and the discrepancies among models, this thesis endeavors to inform future adaptation and mitigation strategies in the region and contribute to validating and improving climate models.

2 Theory

This thesis section presents background information and theory regarding the climate system, aerosols properties, aerosol absorption, black carbons climate interactions, black carbon emissions in Asia, and Earth system models and climate projections.

2.1 The Climate System

In 1901, Herbertson clearly distinguished between weather and climate, stating that "Climate is what we expect, weather is what we get" (Herbertson, 1901, p. 118). Weather is the constantly changing state of the atmosphere, characterized by temperature, wind, precipitation, clouds, and more. This weather results from rapidly developing and decaying weather systems, such as mid-latitude low- and high-pressure systems with their associated frontal zones, showers, and tropical cyclones (Baede et al., 2001). On the other hand, climate refers to the typical weather patterns of a specific geographic area, including the statistical average and its fluctuations over a defined period, typically 30 years, and location (Boucher, 2015b). The climate is dynamic and can shift from one season to another, year after year, and even over extended periods, like during the Ice Ages.

The climate involves the atmosphere, land surface, hydrosphere, cryosphere, and biosphere. Each component shapes the climate system (see Fig. 2.1), while their interactions further influence the different climates. Earth's climate can be categorized into zones based on climate variables better to understand the diverse climatic conditions in various regions. One classification system commonly used is the Köppen-Geiger climate system (Köppen, 1936). It provides a simplified explanation based on precipitation and temperature that divides climates into tropical, arid, temperate, cold, and polar zones (Peel et al., 2007). Various factors, such as latitude, proximity to the sea, vegetation, and topography, contribute to climate variability within these zones (Baede et al., 2001). Furthermore, external factors like atmospheric composition, solar radiation, and volcanic activity can also impact the balance of energy within our atmosphere (Beck et al., 2018).

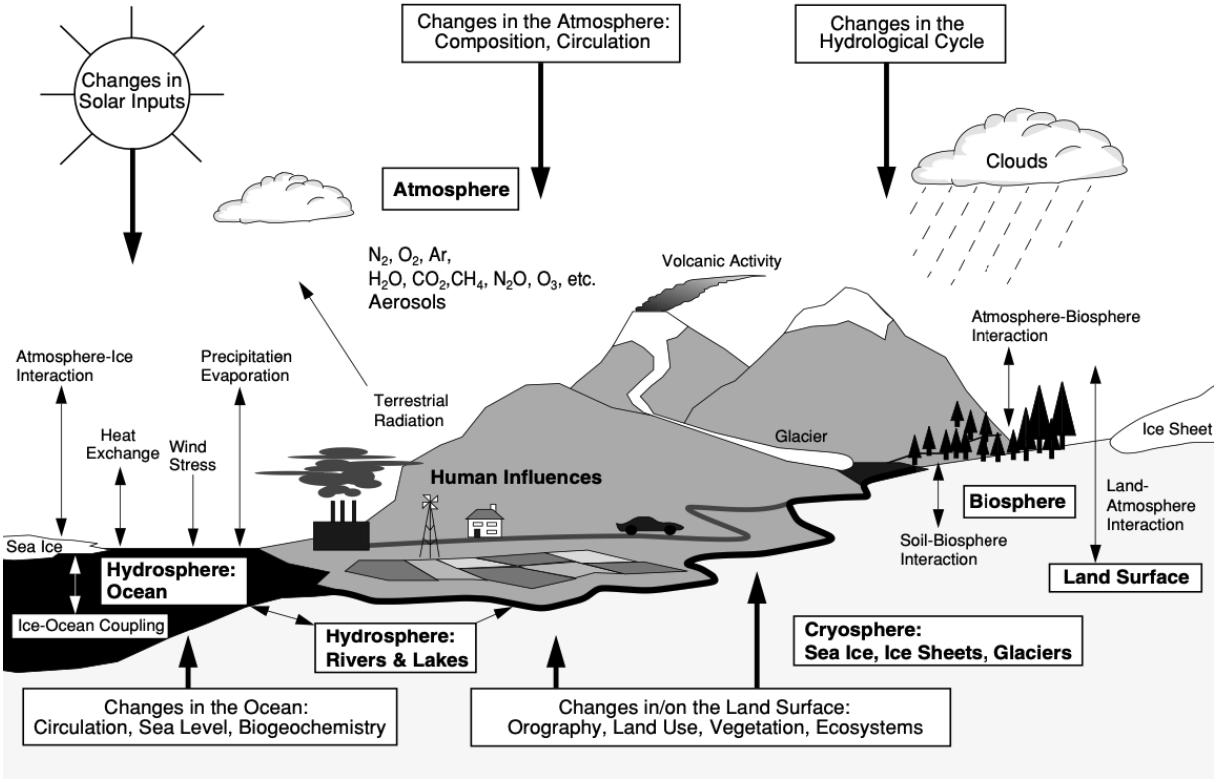

Figure 2.1: Schematic representation of the components (bold writing), processes, and interactions (thin arrow) of the global climate system and some aspects that may change (bold arrows). The figure is taken from Baede et al. (2001).

2.1.1 THE ATMOSPHERE

The atmosphere and the ocean are among the most essential components of the climate system (Boucher, 2015b). The air moves horizontally and vertically, creating weather patterns and shaping climate properties. The atmosphere mainly comprises nitrogen and oxygen, which make up 99% of its volume. The remaining 1% includes trace gases, the most significant being argon, carbon dioxide, water vapor, ozone, and methane (Ramachandran, 2018). The Earth's atmosphere comprises several distinct layers extending from the surface to the top of the atmosphere (TOA). These layers are the troposphere, stratosphere, mesosphere, and thermosphere. With increasing altitude, air density and pressure decrease while temperature varies (Boucher, 2015b), as shown in Figure 2.2.

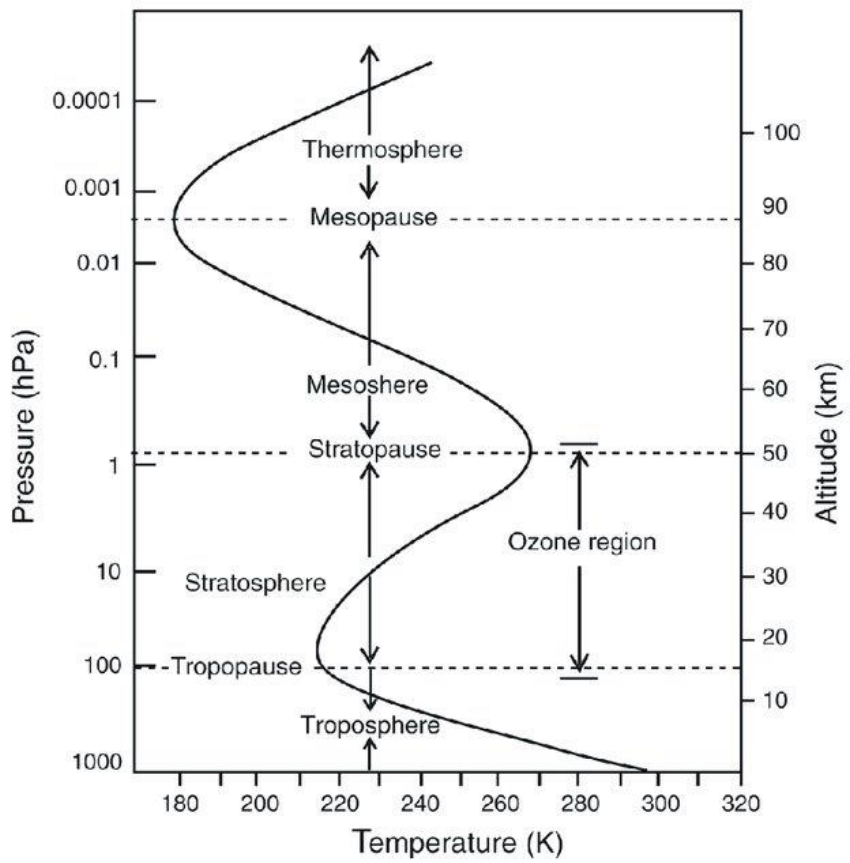

Figure 2.2: Visualization of the different distinct layers in the atmosphere, with the line showing the approximate temperature (K) for different pressure levels (hPa) and altitudes (km). The figure is taken from Mohanakumar (2008).

The troposphere is the layer of the atmosphere closest to the Earth's surface. It contains the majority of the atmosphere's mass and water vapor, which is responsible for cloud formation (National Geographic, 2023). As air ascends through this layer, it cools, resulting in convection. The stratosphere is a distinct layer that begins at the tropopause and extends up to approximately 50 km altitude. In this layer, the temperature rises while the air density decreases. The ozone layer is situated within the stratosphere (Boucher, 2015b). Further, the temperature decreases with altitude as it enters the mesosphere up to about 90 km, reaching the thermosphere, where the temperature increases until the TOA.

The Earth's energy balance is established by the amount of incoming and outgoing radiation in the TOA (IPCC, 2021). As solar radiation enters, reflected shortwave radiation and terrestrial longwave radiation exit the atmosphere. In a steady-state climate, the incoming and outgoing radiation components are in equilibrium, although fluctuations arise from both internal climate variability and anthropogenic forcing, causing energy imbalance (Brown et

al., 2014; Palmer & McNeall, 2014). The presence of gas molecules or particulate matter in the atmosphere causes solar radiation to be absorbed or scattered but allows both solar and terrestrial radiation to pass through. Changes in the abundance of these forms of matter can impact the Earth's energy balance and atmospheric stability (Boucher, 2015b).

The radiation from the sun, while interacting with Earth's surface and atmosphere, helps determine the vertical profile of atmospheric temperature and, therefore, its stability or instability. As air ascends or descends vertically, it cools or heats; these changes in temperature relative to altitude are called adiabatic processes, and they determine the state of the atmosphere (Almethen & Aldaithan, 2017). Air descending from the atmosphere creates high atmospheric pressure, resulting in clear skies and predictable weather conditions. Conversely, when air ascends, it generates low atmospheric pressure, which causes the air to cool and condense into water vapor, leading to cloud formation and an increased probability of precipitation.

2.1.2 The Hydrological Cycle

Despite its small presence, comprising only about 0.25% of the total atmospheric mass, water plays a fundamental role in the climate system (Stevens & Bony, 2013). Water movement is tracked throughout the different components of the Earth's climate system through the intricate hydrological cycle (Chahine, 1992).

Figure 2.3 illustrates the water evaporation process from both ocean and continental surfaces. The water then undergoes multiple cycles of condensation and evaporation in the atmosphere before eventually returning to Earth as precipitation. Water vapor (gas phase) is present in the atmosphere and can be found in clouds containing both liquid and solid water phases. The interaction between water vapor, clouds, and solar and terrestrial radiation is significant. Additionally, biogeochemical cycles, such as carbon, nitrogen, and sulfur, impact the atmosphere's chemical composition and the marine and terrestrial ecosystems (Boucher, 2015b).

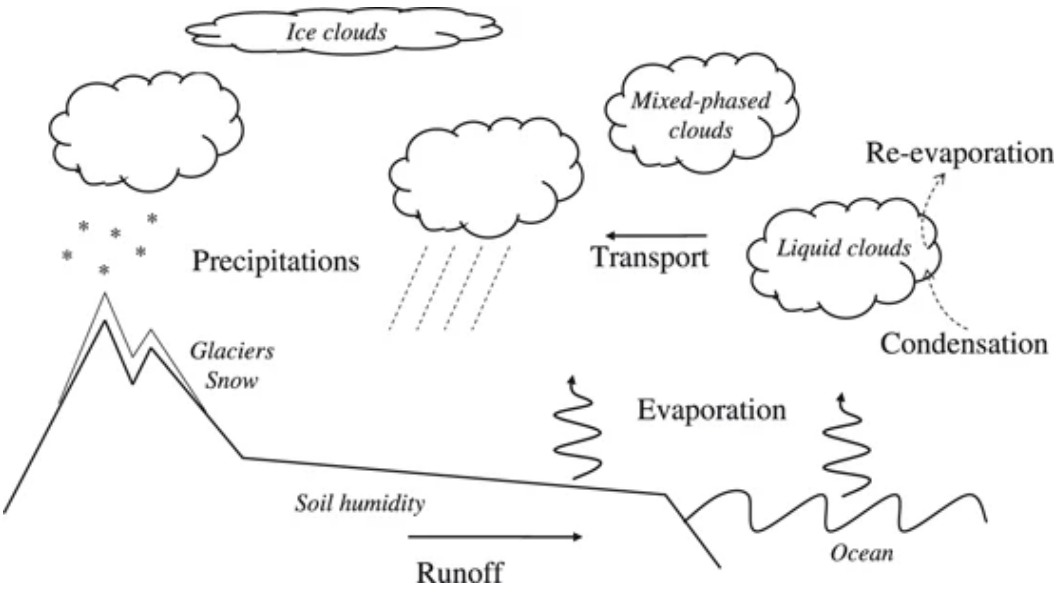

Figure 2.3: Schematic of the hydrological cycle in the climate system. The figure is taken from Boucher (2015b).

Precipitation can take the form of rain, snow, or graupel. Various factors influence precipitation, including global warming, changes in land use, human water consumption, and atmospheric composition (Tang, 2020). Globally, precipitation is constrained by the atmospheric energy balance, such that the latent and sensible heat fluxes are balanced by net atmospheric radiative cooling (Allen & Ingram, 2002; Pendergrass, Angeline G. & Hartmann, 2014; Richardson et al., 2018). Hence, the response of precipitation to climate forcing can be split into two phases: the fast response, a rapid adjustment of the troposphere and stratosphere to the direct change in energy balance caused by a climate forcing agent (e.g., GHGs, aerosols), and the slow response, which is driven by the change in surface temperature (Andrews et al., 2010; Bala et al., 2010; Richardson et al., 2018; Samset et al., 2016). Various climate change drivers perturb the TOA, atmospheric, and surface energy balance in distinct ways. Aerosols, for example, scatter and absorb radiation in the atmosphere, making them influential factors in all these energy balances. Consequently, they are estimated to be essential in disturbing the regional hydrological cycle (Andrews et al., 2010; Ramanathan et al., 2001).

2.1.3 CLIMATE CHANGE

Climate change refers to significant and long-lasting variations in the climate's mean state or variability (Baede et al., 2001). While natural factors like solar irradiance and volcanic eruptions have historically played a role in global climate changes (Zhang, 2020), human activities such as the burning of fossil fuels, deforestation, industrial processes, and agricultural practices have become significant contributors to greenhouse gas (GHG) emissions (Yoro & Daramola, 2020). These emissions alter the Earth's energy balance and cause global warming (Trenberth, 2018), which has significant implications for the climate. There is compelling evidence of rapid climate change, including ocean warming and acidification, ice melting, rising sea levels, and increased extreme weather events such as heatwaves, wildfires, extreme precipitation, and flooding (UNCCS, 2019).

Accurately assessing the impact of changes in the Earth's atmosphere is crucial in measuring global warming and climate change. Radiative forcing (RF) is a valuable tool for estimating these changes, which is expressed in Watts per square meter (Wm^{-2}) (Myhre et al., 2013; Boucher et al., 2013; Forster et al., 2016). Essentially, RF refers to the perturbation of the global energy balance caused by a change in the climate system before any response in temperature or other climate processes takes place (Samset, 2016). These perturbations can arise from natural and anthropogenic sources, including changes in the concentration of well-mixed GHGs like CO_2, CH_4, N_2O, and SF_6 (Collins, W. D., 2019). The respective RF of these GHGs for 2010-2019 are 0.8 Wm^{-2}, 0.5 Wm^{-2}, 0.1 Wm^{-2}, and 0.1 Wm^{-2}, relative to 1850-1900 (Forster, P. et al., 2021). In addition to these factors, other perturbations arise from aerosol burdens, land use characteristics, solar activity, and volcanic eruptions.

The global warming observed has been attributed to the presence of these GHGs in the atmosphere, contributing to a range of 1.0°C to 2.0°C. However, aerosols have partially offset global warming by contributing to a cooling of about 0.0°C to 0.8°C (IPCC, 2023).

2.2 AEROSOLS

Aerosols refer to a collection of particles that are suspended in the atmosphere (Samset, 2016). These particles vary in their physical, chemical, and optical properties, and they can be found from the Earth's surface up to the top of the atmosphere (TOA) at an altitude of about 40 km (Carslaw, 2022a). Aerosol particles impact many aspects of the environment, such as air quality and weather patterns. The term aerosol, which refers to the particles and the suspending gas, is frequently used in this thesis in its plural form to mean 'aerosol particles.'

Aerosols can exist in liquid, solid, or mixed phase states and range from a few nanometers to several tens of micrometers. Due to the significant heterogeneity in aerosol sources, their atmospheric concentration varies. They have a relatively short lifetime of a few hours to a few weeks, which depends on their size, chemical composition, the location of emission, and season (Boucher, 2015a).

2.2.1 AEROSOL CLASSIFICATION

Characterizing individual aerosols is difficult due to the unpredictable variability of their amount and properties. Instead, it is helpful to describe a population of aerosols. This thesis uses Boucher's (2015a) classification of atmospheric aerosols: primary, secondary, and by origin.

Primary aerosols, such as sea spray, mineral dust, or smoke from incomplete combustion or forest fires, are emitted directly into the atmosphere. Secondary aerosols form through the condensation of atmospheric components, such as sulfate from industrial discharges or volcanic sources, rather than originating from direct particulate emissions (Ramachandran, 2018). We also differentiate between natural and anthropogenic origin. The natural sources include emissions from the ocean, soils, vegetation, fires, and volcanoes. Examples are salt particles from sea spray and mineral dust swept up by winds and soot from wildfires. On the other hand, anthropogenic aerosols are generated by human activities such as the combustion of fossil fuels, biofuels, industrial activities, and domestic activities. The primary anthropogenic aerosols are sulfate and nitrate compounds, organic aerosols, and BC (Samset, 2016).

2.2.2 PHYSICAL PROPERTIES OF AEROSOLS

This section introduces aerosol particles' physical, chemical, and optical properties and their spatial distribution and variability.

Understanding aerosol concentration and chemical composition in the atmosphere goes beyond identifying their sources. Once airborne, aerosols are subject to a variety of processes, such as transportation and dry deposition due to global wind patterns, wet deposition due to precipitation, convection due to temperature, and condensation, dissolution, and coagulation due to humidity, see Figure 2 for an example with BC. These processes cause aerosols to have a spatially and temporally heterogeneous concentration and distribution in the atmosphere (Boucher, 2015a; Carslaw, 2022b).

Aerosol concentrations typically range from 100-1000 cm^{-3}, with most particles measuring 10-200 nm in diameter (Carslaw & Pringle, 2022). Concentrations also vary vertically, where they are generally more common in the atmospheric boundary layer than in the troposphere (Boucher, 2015a). Aerosols in the troposphere include sea salt, mineral dust, nitrate, sulfate, and organic and black carbon. Meanwhile, the stratosphere primarily contains sulfate aerosols. The aerosol concentrations vary according to closeness to their emission source, region, altitude, and season (Ramachandran, 2018).

It is essential to determine the optical properties of aerosols to understand their impact on the Earth's radiation budget. In the visible spectrum, scattering is the dominant interaction between radiation and aerosols (Kokhanovsky, 2008). However, some aerosols also can absorb radiation.

2.2.3 Aerosols-Radiation Interactions

Atmospheric aerosols significantly impact the climate by causing RF directly through scattering and absorbing radiation in the atmosphere, thus altering the planetary albedo (Twomey, 1977). They have an indirect effect by acting as cloud condensation nuclei (CNN) or ice-nucleating particles (INPs), altering cloud properties such as reflectivity and lifetime through microphysical processes (Li, J. et al., 2022). Aerosols can also modify cloud properties without directly acting as CNN and INPs. This is called the semi-direct effect, whereby they absorb solar radiation, increasing the ambient air temperature. This, in turn, results in the evaporation of cloud droplets (Rao, Sofiya & Dey, 2020). Moreover, aerosols can deposit on snow and ice surfaces, indirectly altering the Earth's albedo (see Fig. 2.4).

These effects can be grouped into three types of interactions: aerosol-radiation interactions (ARI), aerosol-cloud interactions (ACI), including both indirect and semi-direct effects, and aerosol-surface interactions. This thesis focuses on ARI and the semi-direct effects of ACI and how they affect Earth's climate, especially precipitation, in response to a reduction of absorbing aerosols.

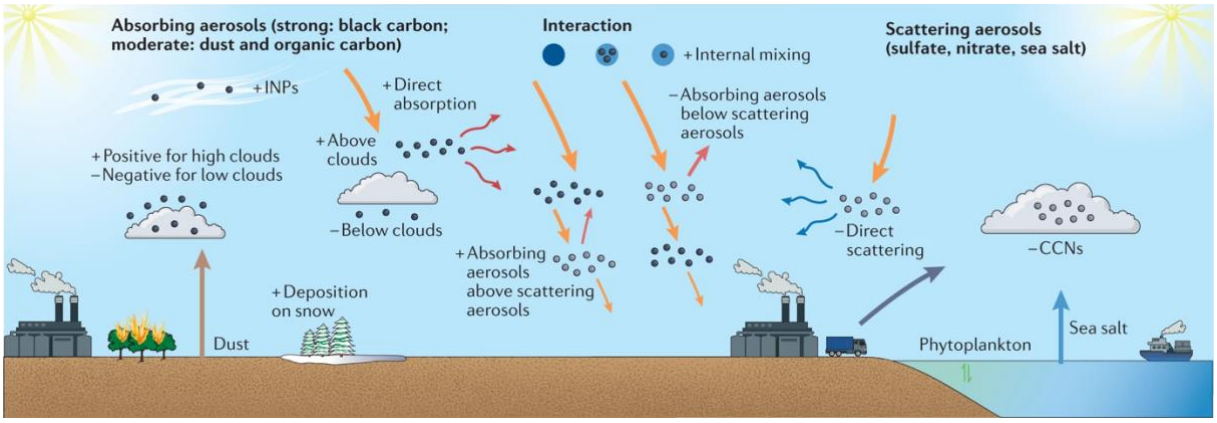

Figure 2.4: Overview of radiative effects of absorbing (dark grey dots) and scattering (light grey dots) aerosols and their interactive effects. This figure is taken from Li, J. et al. (2022).

Aerosol scattering and its effect on climate is the ARI best understood. Shortwave radiation is scattered in various directions by mainly sea salt, sulfate, and nitrate aerosols, resulting in a cooling effect on the climate system by reflecting more radiation (Li, J. et al., 2022; Ramanathan et al., 2001). However, high surface albedo and clouds can mitigate this effect (Liao & Seinfeld, 1998; Thorsen et al., 2020). Aerosols have unique directional scattering and

polarization properties. Non-spherical particles scatter light more efficiently and exhibit shape-dependent polarization. In global climate modeling, aerosols are generally considered homogeneous spheres (Li, J. et al., 2022), and optical processes, size distributions, growth, and aging factors are considered (Mann et al., 2014). Differential equations describing the interactions of incoming shortwave radiation with aerosols in the atmosphere are solved based on Mie theory (Samset, 2016). Aerosol absorption is a phenomenon in which certain aerosols, predominantly black carbon, absorb incoming shortwave radiation (Bond et al., 2013). This is presented more thoroughly in section 2.3 of this thesis.

The changes in global aerosol abundances caused by anthropogenic activities alter the natural aerosol radiative effect (Carslaw, 2022a). Quantifying the RF caused by aerosols within the climate system is achieved through the use of aerosol effective radiative forcing (ERF), which is defined as the change in TOA flux following a perturbation within the climate system (Forster, P. M. et al., 2016). The IPCC AR6 has used observational and modeling evidence to estimate a 1750 to 2015 global mean aerosol ERF of -1.3 (-2.0 to -0.6) Wm^{-2} (medium confidence), and the ERF due to ARI to be -0.3 °± 0.3 Wm^{-2} (5-95 % credible interval) (IPCC, 2021).

The presence of additional atmospheric aerosols leads to an increase in the scattering and absorption of radiation. This, in turn, alters the Earth's radiative balance, consequently impacting the climate (Li, J. et al., 2022). For instance, it changes the vertical temperature profile of the atmosphere, thereby triggering rapid atmospheric adjustments that can affect atmospheric stability, relative humidity, and, consequently, cloud formation (Bond et al., 2013).

2.2.4 Aerosol Measurement Techniques

Accurately estimating aerosol RF requires comprehensive information on their loadings, optical properties, and microphysical characteristics (Bellouin et al., 2013). Given aerosols' significant inhomogeneous spatial and temporal variability, remote sensing is an important method to obtain insight into this information (IPCC, 2013; Ramanathan et al., 2001; Shin et al., 2019).

Remote sensing is the measurement of an object's characteristics from a distance using ground-based or satellite-based methods. Passive remote sensing categorizes observations of natural electromagnetic radiation into extinction/scattering of solar radiation and absorption/emission of terrestrial radiation. For example, measurements of solar radiation extinction in the visible spectrum can be retrieved using sun photometers or spectrometers. Observations in the infrared range provide insights into vertical absorption and emission in the atmosphere (Boucher, 2015c), as well as measurements of aerosol absorption via in situ instruments at long-term surface stations and during aircraft field operations (Samset, B. H. et al., 2018).

The Aerosol Robotic Network (AERONET) is an example of a ground-based monitoring system that utilizes sun-sky radiometers to provide long-term observations of Aerosol Optical Depth (AOD) and Aerosol Absorption Optical Depth (AAOD), among other parameters (Holben et al., 1998; Holben et al., 2001; Shin et al., 2019). AOD, derived from the solar radiation reflected into space, is the height integral of the aerosol extinction coefficient. AAOD is retrieved from observations of the column aerosol loading of absorbing aerosols, which can be ambiguous if multiple types of absorbing aerosols, such as BC, BrC, and mineral dust, are present in a mixed aerosol plume (Shin et al., 2019).

2.3 Absorbing Aerosols

Due to their diverse chemical and optical compositions, various aerosols can absorb shortwave radiation in the atmosphere. Amongst these, BC stands out as the primary contributor. While brown carbon (BrC) and mineral dust can absorb UV radiation, their absorption ability becomes insignificant beyond 600 nm (Bergstrom et al., 2007; Samset, B. H. et al., 2018). The ability of an aerosol particle to absorb radiation depends on size, optical properties, and morphology (Samset, 2016).

In contrast to the global mean aerosol RF, aerosol absorption leads to a positive RF in the climate system. It heats the particles and emits longwave heat radiation to the ambient air, contributing to atmospheric warming. Several factors influence the impact of absorption, including surface albedo, cloud cover, location, and altitude. At the surface, the cooling effect still dominates as aerosol heating occurs higher in the atmosphere (Satheesh & Ramanathan, 2000).

Absorbing aerosols' vertical distribution is also crucial in determining their radiative impact, especially in sparsely reflective surfaces and clear skies. When located at higher altitudes, they have a more pronounced warming effect (Haywood & Ramaswamy, 1998; Li, J. et al., 2022). However, a lower layer of aerosols on highly reflective surfaces can lead to a more significant warming effect (Mishra et al., 2015).

The extent to which aerosols absorb shortwave energy in the atmosphere is subject to high uncertainty. It can be inferred through an inversion of measurements from sun-sky photometers at AERONET stations, although this method has limitations and uncertainties (Giles et al., 2012; Samset, 2022). The uncertainties primarily arise from the fact that observations of aerosol absorption are still essentially unconstrained, as current photometric satellite sensors lack the necessary capability to measure it with accuracy (Samset, 2022; Samset, B. H. et al., 2018; Sand, M. et al., 2021).

2.3.1 Characteristics of Black Carbon

This thesis focuses on black carbon (BC) in soot and its impact on the climate system. BC is formally defined as an ideally light-absorbing substance composed of carbon (Petzold et al., 2013).

BC emissions are a result of the incomplete combustion of mainly fossil fuels (diesel and coal) but also biofuels (wood, dung, and crop residue) and biomass (deforestation and crop residue burning) (Andreae, Meinrat O. & Crutzen, 1997). BC has a representative mass absorption cross-section (MAC) value of 7.5 m^2g^{-1} at a wavelength of 550 nm (Samset, B. H. et al., 2018), dependent on whether it is freshly generated or aged and coated. BC particles near their source typically have a primary spherule diameter of 10-50 nm, with fractal dimensions of 1.5-2.2 (Liu, D. et al., 2020). This refractory aerosol type has a high vaporization temperature, reaching nearly 4000 K (Bond et al., 2013).

BC particles vary in shape and structure depending on their source of origin and the combustion temperature (Andreae, M. O. & Gelencsér, 2006; Mikhailov et al., 2006). Following their emission, BC particles undergo physical and chemical transformations as they age and interact with other atmospheric components, which result in morphological and hygroscopic changes. The lifetime of BC particles and the atmospheric conditions to which they are exposed induce spatial and temporal variations in their optical properties (Samset, B. H. et al., 2018). It is primarily removed from the atmosphere through wet or dry deposition (Bond et al., 2013).

BC particles are not as effective as cloud condensation nuclei (CCN) when freshly emitted due to their hydrophobic nature. But, as they age and accumulate soluble mass, they grow and become more hygroscopic, enhancing their CCN activity (Bond et al., 2013). They are generally found close to their emission source in mixed aerosol plumes, along with other particles typically co-emitted with BC (Petzold et al., 2013).

Anthropogenic sources of BC are mainly concentrated in urban areas and tropical regions where solar irradiance is the highest (Ramanathan & Carmichael, 2008). The dome effect of BC in these regions interacts with the planetary boundary layers, leading to extreme haze pollution (Ding et al., 2016), which often occurs in megacities like Beijing or New Delhi (see

Fig. 1.1). Nevertheless, these emissions are not confined to these regions and can be transported long distances.

BC particles are among the most significant aerosol species that contribute to the aerosol direct effect on the climate with their unique ability to absorb visible light (Samset, B. H. et al., 2018). BC also contributes to the aerosol semi- and indirect effect (Bond et al., 2013).

2.3.2 Black Carbon Influence on Climate Properties

BC is known to be the second-largest warming agent in the atmosphere, immediately after GHGs (Chen et al., 2023). Over the last decades, it has become clear that absorbing aerosols significantly impacts global and regional climate, particularly the hydrological cycle (Ramanathan et al., 2001). Figure 2.5 shows an illustration of the various ways in which BC interacts with and affects the climate system.

BC has opposing effects of adding energy to the atmosphere but initially reducing it at the surface, unlike the greenhouse effect of CO_2 that leads to a positive RF of the atmosphere and the surface (Ramanathan & Carmichael, 2008). BC alters the RF through complex processes, ultimately contributing to a net reduction in planetary albedo (Mikhailov et al., 2006; Moorthy et al., 2005). These processes include the absorption of solar radiation reflected by the surface-atmosphere-cloud system (direct effect) and dry and wet deposition on snow and ice. When BC particles are located above clouds, they may also interact with reflected radiation, which causes the average aerosol absorption to increase with altitude. However, below a thick cloud, aerosol absorption is weakened (Bond et al., 2013).

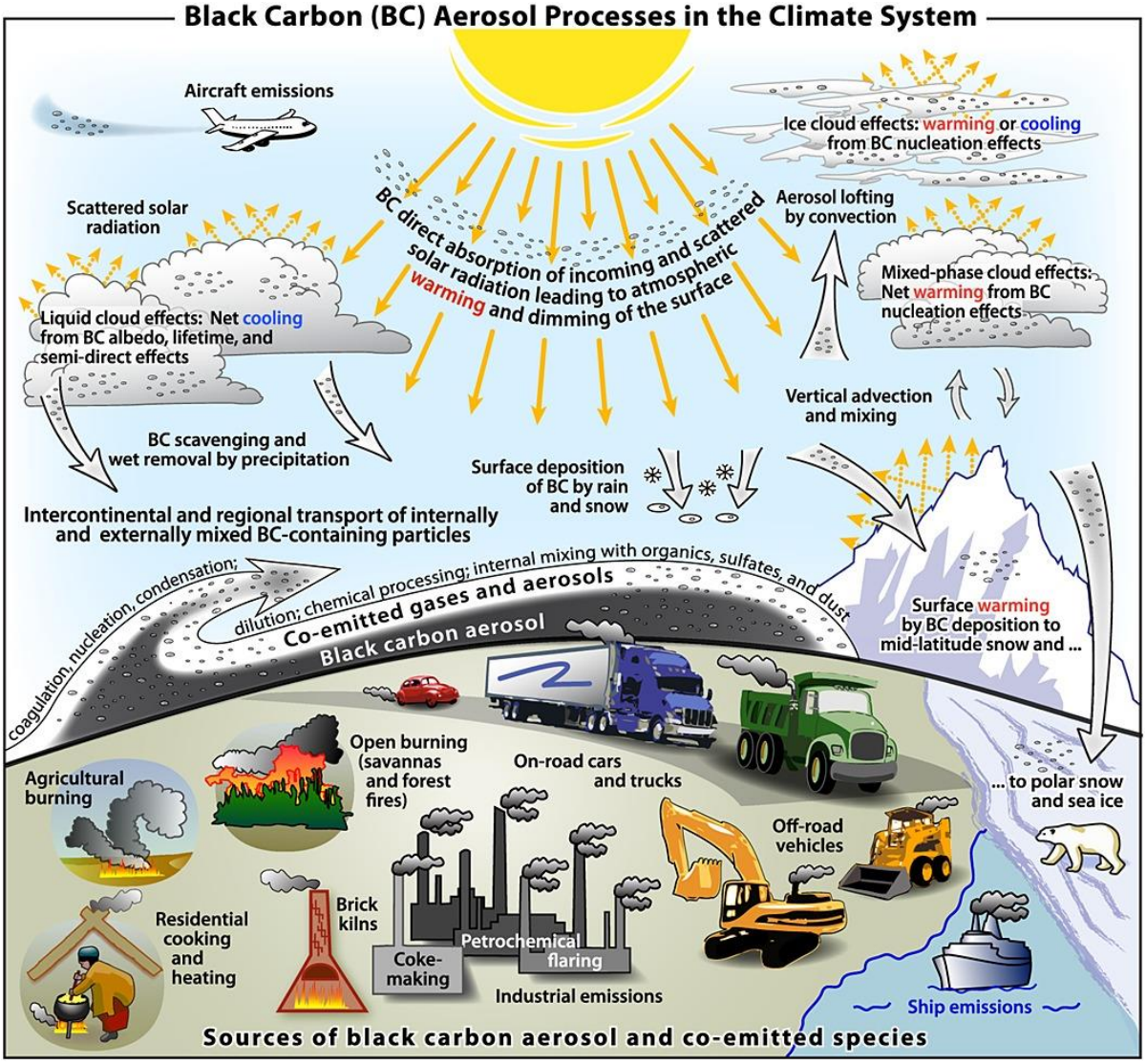

Figure 2.5: Schematic overview of the primary BC emission sources, how it is distributed in the atmosphere, and the processes and effects in the climate system. This figure is taken from Bond et al. (2013).

Additionally, soot inside cloud drops and ice crystals (indirect effect) can decrease the albedo of clouds by enhancing absorption by droplets and ice crystals. The mentioned processes result in a positive forcing at the TOA, subsequently increasing atmospheric heating. It is important to note that BC initially cools the surface due to its ability to function as an aerosol mask (Ramanathan & Carmichael, 2008). But over time, the warm air in the atmosphere flows downwards, resulting in BC having a net warming effect on the surface.

BC can also alter cloud properties without occupying the cloud droplets and ice crystals (semi-direct effect). This effect can occur in two distinct ways. Firstly, BC can heat the ambient air while reducing radiation that reaches the surface. This stabilizes the atmosphere and lessens convection, lowering the potential for cloud formation. Secondly, BC can increase

atmospheric heating and reduce the relative humidity, which hinders the formation of clouds and may promote cloud evaporation (Myhre, 2013).

The BC-induced atmospheric heating tends to slow down the hydrological cycle (Pendergrass, A. G. & Hartmann, 2012; Ramanathan & Carmichael, 2008; Ramanathan et al., 2001). The process, known as rapid precipitation change, suppresses precipitation formation and alters cloud formation (Sand, Maria et al., 2020). This is due to the competition between the latent heat released during condensation and the atmospheric heating rate resulting from the absorption of aerosols (Samset, 2022). Furthermore, these effects may trigger a positive feedback loop of aerosol climate effects by decreasing aerosol wet deposition.

Temperature gradients between BC-polluted regions and their surroundings also cause climatic effects, which ultimately can cause shifts in regional circulation patterns (Li, J. et al., 2022), such as the Asian monsoon (Bollasina et al., 2014; Menon et al., 2002). BC has been proposed to contribute to inducing latitudinal gradients in tropospheric heating over the Asian region during the pre-monsoon season, also called the "Elevated heat pump" effect (Lau, K. M. et al., 2006), which may result in changes in arrival and duration of the ASM (Das et al., 2020; Lau, K.-M. & Kim, 2006).

2.4 South and East Asian Climate Characteristics and BC Emission Trends

As previously stated, anthropogenic aerosol emissions over Asia have changed rapidly in composition and spatial distribution in the last decade (Samset et al., 2019). The primary sources of BC emissions in East Asia are attributed to coal-burning industries, followed by traffic and biomass burning (Ramachandran & Rupakheti, 2022). Meanwhile, traffic and burning biomass and refuse are significant sources of BC emissions in South Asia, with industrial activities following closely (Klimont et al., 2017). The considerable decrease in East Asia has caused a dipole pattern to form over Asia, while South Asia has experienced an increase (Ramachandran et al., 2022). The rapid change witnessed is attributed to the combined effects of population and economic growth and greater energy consumption, which contribute to increased emissions. However, cleaner technology and fuels reduce emissions (Bond et al., 2013).

2.4.1 THE ASIAN MONSOON

Monsoon climates are defined by distinct wet and dry seasons, a reversal of seasonal winds, and a sudden onset of seasonal monsoon rainfalls (Lau, W. K. M., 2016). The Asian monsoon is an extensive atmospheric circulation system that arises from the seasonal solar heating cycle over Asia, creating a temperature gradient between the land and ocean (Li, Z. et al., 2016). During boreal summer, the Asian monsoon carries heat and moisture across the Indian Ocean and the tropical western Pacific to the Indian subcontinent and southeastern Asia, even up to northern China and Japan (Cheng et al., 2016). The seasonal differences in precipitation occur due to the land-sea gradient and the influence of northeasterly and southwesterly winds. These are caused by surface turbulent heat fluxes, as well as latent heating from rainfall and deep convection (Li, Z. et al., 2016; Ramachandran et al., 2020; Wang & Ding, 2008). The circulation system is also distinguished by the unique influence of the Tibetan Plateau (Wu, G. et al., 2012), which plays a significant role in driving the circulation of the monsoon and the convergence of moisture patterns. Elevated thermal and mechanical forcing from the plateau contributes to the system's characteristic features, such as its timing and duration (Yanai & Wu, 2006; Ye & Wu, 1998).

The Asian monsoon displays a sensitivity to many factors: GHGs, the interhemispheric temperature gradient, the position of the intertropical convergence zone (ITCZ), and the atmospheric wave pattern over Eurasia (Polson et al., 2014; Wilcox et al., 2020), as well as local and remote aerosol variations (Bollasina et al., 2014; Undorf et al., 2018).

The ITCZ is an essential component of the climate system near the equator. A narrow region of rising air and intense precipitation characterizes it. It plays a significant role in shaping the Asian monsoon system and contributes to a substantial portion of global rainfall. Its movements are influenced by the seasonal cycle of solar insolation and cause oscillations north and south across the equator, closely linked to monsoon circulations (Bordoni & Schneider, 2008). Moisture convergence from the cooling northerly and southerly trade winds that collide near the equator drives the ITCZ (Byrne et al., 2018).

The rainfall provided by the ITCZ and monsoon plays a crucial role in sustaining agriculture, energy, industry, and local water resources in Asia, and almost half of the world's population is dependent on it (Bollasina et al., 2011; Herbert et al., 2022).

2.5 Earth System Models and Climate Projections

Climate models are essential for researchers to simulate and quantify uncertainties in the intricate dynamics of the Earth's climate on a global and regional scale (Guilyardi et al., 2013).

Global Climate Models (GCMs) are sophisticated mathematical representations replicating Earth's climate system by considering its major components, such as the atmosphere, ocean, and land surface (Ganopolski, 2019). These models employ a three-dimensional grid of cells to emulate the physical characteristics of the climate system, including atmospheric circulation, temperature, and precipitation, among other factors (Randall et al., 2007). Furthermore, the model's components exchange heat, water, and momentum fluxes, interacting as a coupled system.

Initially, climate models solely described physical processes in the atmosphere, ocean, and land surface. However, factoring in geochemical, biochemical, and biological processes is essential for precise future projections. Accurate carbon cycle, atmospheric chemistry, and ice sheet modeling are also critical (Ganopolski, 2019). The most comprehensive method for studying climate change involves earth system models (ESMs) incorporating all these components.

2.5.1 CMIP6

The Coupled Model Intercomparison Project (CMIP) was launched twenty years ago by the World Climate Research Programme's (WCRP) Working Group on Coupled Modelling (WGCM). Over six phases (CMIP6), it has grown into a significant multi-model research initiative that has become an essential component of climate change assessments (IPCC, 2013).

The primary objective of the CMIP is to enhance the understanding of the Earth's global climate system. This is achieved by designing, distributing, and analyzing past, present, and future global climate model simulations. This further assesses model performance and provides future projections by quantifying perturbations. Using idealized experiments (MIPs), such as the Aerosols and Chemistry Model Intercomparison Project (AerChemMIP), is a valuable approach to enhancing understanding of model responses (Eyring et al., 2016).

AerChemMIP, endorsed by CMIP6, aims to assess the impacts of aerosols and their precursors on climate and air quality, particularly for near-term climate forcers (NTCFs) (Collins, W. J. et al., 2017). This is accomplished through targeted simulations with climate models that quantify the climate effects of interactive aerosols and atmospheric chemistry. AerChemMIP further aims to examine the surface temperature and precipitation changes associated with future NTCF mitigation efforts, focusing on experiments on aerosols and their global and regional effects (Collins, W. J. et al., 2017).

2.5.2 Shared Socio-economic Pathways (SSPs)

The experiments in AerChemMIP are built upon Shared Socio-economic Pathways (SSPs) created from socioeconomic and climate conditions (O'Neill et al., 2016). The SSPs involve varying levels of pollution control – weak, medium, and strong - that progress differently for high, medium, and low-income countries (refer to Table 2.1). These levels correspond to different approaches to adhering to the current legislation emission (CLE) and maximum technically feasible reduction (MTFR) (Rao, Shilpa et al., 2017). CLE denotes emission factors that rely on implementing current environmental legislation up to 2030 and sufficient institutional support. Meanwhile, MTFR represents emission factors that presume the complete adoption of "best available technology" by 2030, without regard for cost but with consideration of the economic lifespan of technologies.

Table 2.1: Qualitative framework for pollution control in the SSPs, taken from Rao, Shilpa et al. (2017).

Policy strength	Policy targets		Technological innovation	Related SSP	Key characteristics of SSPs
	High income countries	Medium and low-income countries			
Strong	Aim for much lower pollutant levels than current targets.	Comparatively quick catch-up with the developed countries.	Pollution control technology costs drop substantially with control performance increasing.	SSP1, SSP5.	Sustainability driven.
Medium	Lower than current targets.	Catch-up with the developed countries, but not as quick as in the "Strong" case.	Continued modest technology advances.	SSP2.	Middle-of-the-road scenario.
Weak	Regionally varied policies.	Trade barriers and/or institutional limitations substantially slow progress in pollution control.	Lower levels of technological advance overall.	SSP3, SSP4.	Fragmentation, inequalities.

This thesis focuses on the future scenario SSP3-7.0 (see Fig. 2.6), also known as "Regional Rivalry," which is a baseline case with a Representative Concentration Pathway (RCP) level of 7.0 Wm^{-2} by 2100 and no climate mitigation policy (Fujimori et al., 2017). The RCPs contain different emissions projections for all long- and short-lived climate forcers, including aerosol and their precursors (Westervelt et al., 2015). SSP3-7.0 has the highest level of SLCFs and "Weak" levels of air quality control measures (Collins, W. J. et al., 2017; Rao, Shilpa et al., 2017), which makes it suitable for detecting significant signals. Weak pollution controls assume delays in implementing CLE and make little progress towards MTFR.

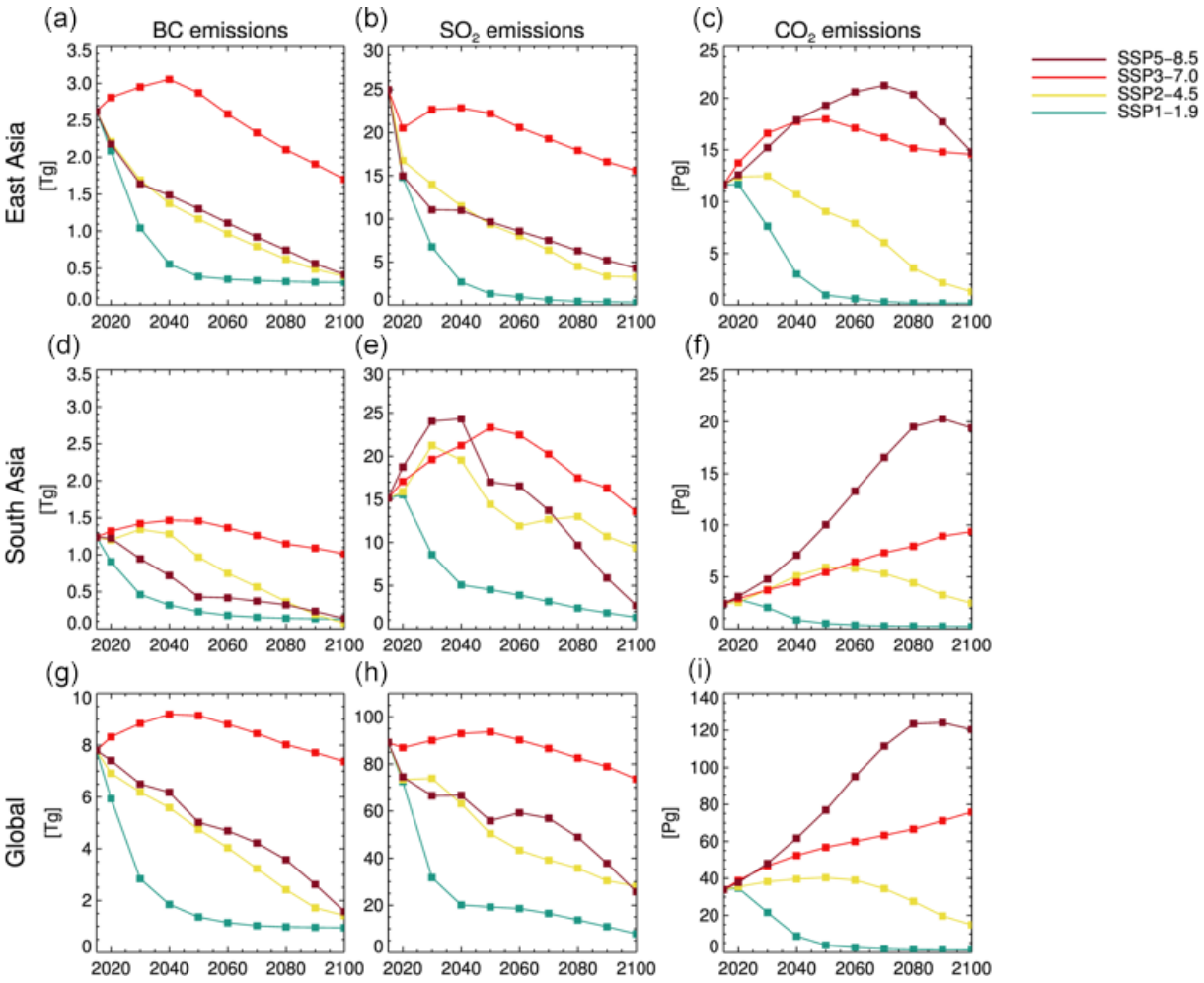

Figure 2.6: An illustration of (a) Black carbon (Tg), (b) sulfur dioxide (Tg), and (c) carbon dioxide emissions over East Asia for different SSPs, with the bright red line representing our chosen scenario SSP3-7.0. (d-f) Emissions over South Asia and (g-i) global emissions. The East Asian region covers 20-40˚N and 100-120˚E, and South Asia covers 5-25˚N and 55-95˚E. The figure is taken from Wilcox et al. (2020).

3 Methods

This study aims to use ESMs to assess the impact of a rapid phaseout of BC emissions on various climate variables in a future scenario. Additionally, it seeks to evaluate discrepancies among the models. Three distinct Earth System Models (ESMs), namely UKESM1.0-LL, MIROC6, and MPI-ESM1.2-HAM, will be employed for this purpose. Anomalies in global, regional, and seasonal variables are visualized, including Aerosol Absorption Optical Depth (AAOD), near-surface air temperature (tas), precipitation (pr), vertical mass flux (omega), and air temperature (ta). The study emphasizes the potential impact of a phaseout of BC emissions on precipitation patterns in South and East Asia, particularly concerning the progression of the ASM.

3.1 Materials and Experiment

The globally gridded datasets are provided in netCDF format and are categorized into two experiments based on the SSP3-7.0 scenario pathway, namely SSP3-7.0-SST and SSP3-7.0-SST-lowBC. From here, they are referred to as ssp370 and ssp370-lowBC. The ssp370 scenario sits in the upper end of the range of future forcing pathways in the coming decades (see Fig. 2.6), characterized by unmitigated forcing, increased aerosol emissions, and a medium to high range of GHG concentrations (O'Neill et al., 2016; Rao, Shilpa et al., 2017; Riahi et al., 2017). The ssp370-lowBC scenario has the same settings and climate mitigation measures but is perturbed by the maximal feasible reductions of air quality policy measures for BC. Differences in climate, ERF, chemical composition, and air quality between the two scenarios will be solely due to these measures (Collins, W. J. et al., 2017). The aerosol emissions are from Rao, Shilpa et al. (2017), and Lund et al. (2020). All available data are used for each experiment.

The ssp370 and ssp370-lowBC scenarios have distinct datasets for each climate model. Furthermore, each climate model has specific datasets for the variables AAOD, tas, pr, omega, and ta, which are analyzed in this study. Table 3.1 overviews the variables and their attributes in the different climate models [1].

Table 3.1: An overview of the simulation variables and their attributes. Necessary updates or clarifications are summarized in the "comments" section. When an attribute is changed in the dataset, the old attribute is listed before the forward slash, and the new attribute is listed after.

Variable	Long name	Standard name	Coordinates	Units	Comments
abs550-aer	Ambient Aerosol Absorption Optical Thickness at 550nm	Atmosphere absorption optical depth due to ambient aerosol particles	Time, longitude (degrees east), latitude (degrees north)	1	AAOD at wavelength 550 nanometers
tas	Near-Surface Air Temperature	Air temperature	Time, longitude latitude, height (meters)	K (Kelvin)/ ºC (Celsius)	Near-surface is usually 2 meters.
pr	Precipitation	Precipitation flux	Time, longitude, latitude	Kg m^{-2} s^{-1} / mm day^{-1}	Includes both liquid and solid phases.
ta	Air Temperature	Air Temperature	Time, longitude, latitude, plev (pressure: Pa)	K (Kelvin)/ ºC (Celsius)	19 plev (pressure levels), positive downwards.
Wap/ omega	Omega (=-dp/dt)	Lagrangian tendency of air pressure/vertical mass flux	Time, longitude, latitude, plev	Pa s^{-1}	Measured at an altitude of 850 and 250 hPa, positive upwards.

[1] Access additional information on the datasets from each climate model through the Earth System Grid Federation (ESGF) search page (https://aims2.llnl.gov/search) or by using the 'further_info_url' global attribute in each CMIP6 netCDF data file.

3.2 MODELS

The analysis is conducted using output data from three different Earth System Models (ESMs) that are a part of the CMIP6 experiment. These models are the United Kingdom Earth System Model 1.0 - Low Resolution (UKESM1.0-LL), which was released in 2018, as well as the Model for Interdisciplinary Research On Climate version 6 (MIROC6) and Max Planck Institute Earth System Model version 1.2 with HAM aerosol model (MPI-ESM1.2-HAM), both of which were released in 2017.

The models' attributes are summarized in Table 3.2. All models are run with prescribed sea surface temperatures (SSTs), or fSST, which means that sea surface temperature and sea ice are held constant at observed levels, and the ocean does not dynamically interact with the atmosphere in the models. Aerosols are computed from emissions, while GHGs have prescribed concentrations.

Table 3.2: ESMs participating in CMIP6 and in this thesis and their specifications. Column 1: Sponsoring institution(s). Column 2: Model names. Column 3: Model version. Column 4: Horizontal grid resolution, model resolution, number of vertical levels, grid top. Column 5: Atmosphere and aerosol component. Column 6: Main reference(s).

Institution, Country, or Region	**Model**	**Version**	**Resolution (km), (lon × lat), Number of levels (L) and Top (km)**	**Atmosphere and Aerosol component**	**Main reference(s)**
MOHC, Met Office Hadley Centre, UK	UKESM1.0-LL	3.1	140 km, (1.875° × 1.25°), 85 L, Top 85 km	MetUM-HadGEM3-GA7.1, UKCA-GLOMAP	(Sellar et al., 2019)
MIROC Consortium, JAMSTEC, AORI, NIES, R-CCS Japan	MIROC6	6	120 km, (1.4° × 1.4°), 81 L, Top 80 km	CCSR AGCM, SPRINTARS	(Tatebe et al., 2019)
HAMMOZ-Consortium Switzerland, Germany, UK, Finland	MPI-ESM1.2-HAM	HAM2.3	170 km, (1.9° × 1.9°), 47 L, Top 80 km	ECHAM6.3, HAM2.3	(Mauritsen et al., 2019), (Neubauer et al., 2019)

To generate statistical information for sensitivity studies, modeling centers conduct experiments using one model with slightly different settings. This set of runs is called an "ensemble" and is categorized into four indices: realization_index (r), initialization_index (i), physics_index (p), and forcing_index (f). These indices distinguish runs of a single CMIP6 experiment that have undergone different perturbations. In this experiment, UKESM's ensemble is labeled "r1i1p1f2", while MIROC and MPI-ESM are labeled "r1i1p1f1".

3.3 SIMULATION DETAILS

The simulations run with the AerChemMIP experiment setup and diagnostics, and the data for the perturbed scenario is generated by the Asia-Pacific Integrated Modeling (AIM) group.

The two future scenario experiments begin in January 2015, and they run to December 2054 (December 2094 for UKESM1.0-LL), following the ssp370 and ssp370-lowBC scenarios for WMGHG (well-mixed GHGs: methane, nitrous oxide, halocarbons) and BC emissions. This period is selected because it is expected to show the most extensive divergence in air quality policies and the most significant reductions in aerosol (Collins, W. J. et al., 2017).

For both the ssp370 scenario and ssp370-lowBC scenario, the simulation calculates the mean over 20-year intervals for the climate variable in question. The anomalies are derived by subtracting the mean of ssp370 from the mean of ssp370-lowBC and then visualized by plotting them on map projections. Curtain plots are utilized for the vertical temperature projections. Plotting and visualizing these anomalies allows for a thorough analysis of interconnections between variables and model comparison.

The analysis is based on a detailed examination of climate variables' anomalies, evaluated with maps at three distinct levels - global, regional, and seasonal. This approach enables a nuanced understanding of climate dynamics and seasonal variability. The scope of the regional analysis is focused on South and East Asia, covering the geographical region that expands from 65˚E to 130˚E and from -10˚S to 40˚N. The analysis of seasons zeroes in December to February (DJF) and June to August (JJA) to observe the seasonal shifts in the monsoon.

3.4 Data Processing and Statistics

Jupyter Notebook, running with Python version 3.11.4, is used extensively for data processing and visualization [2] (see Appendix A). A statistical significance test is performed to ensure the robustness of observed trends. Specifically, the annual means of the ssp370 and ssp370-lowBC datasets undergo a student's t-test to determine that the differences at each grid point are statistically significant at the 95% confidence level. Significant differences are highlighted as small grey dots on the maps, while non-significant grid points are not visually emphasized. This approach is utilized for all variables except AAOD, as this variable demonstrates too many statistically significant differences. Here, the non-significant points are highlighted. The main objective of this methodology is to distinguish regions of significant change from those with less robust evidence.

[2] The code is available from: https://github.com/julnav2010/Master-Thesis-Navdahl/tree/main

4 Results

This section presents the key results of the simulations. From here, the models are referred to as UKESM, MIROC, and MPI-ESM, and using the term "significant" indicates statistical significance, not magnitude.

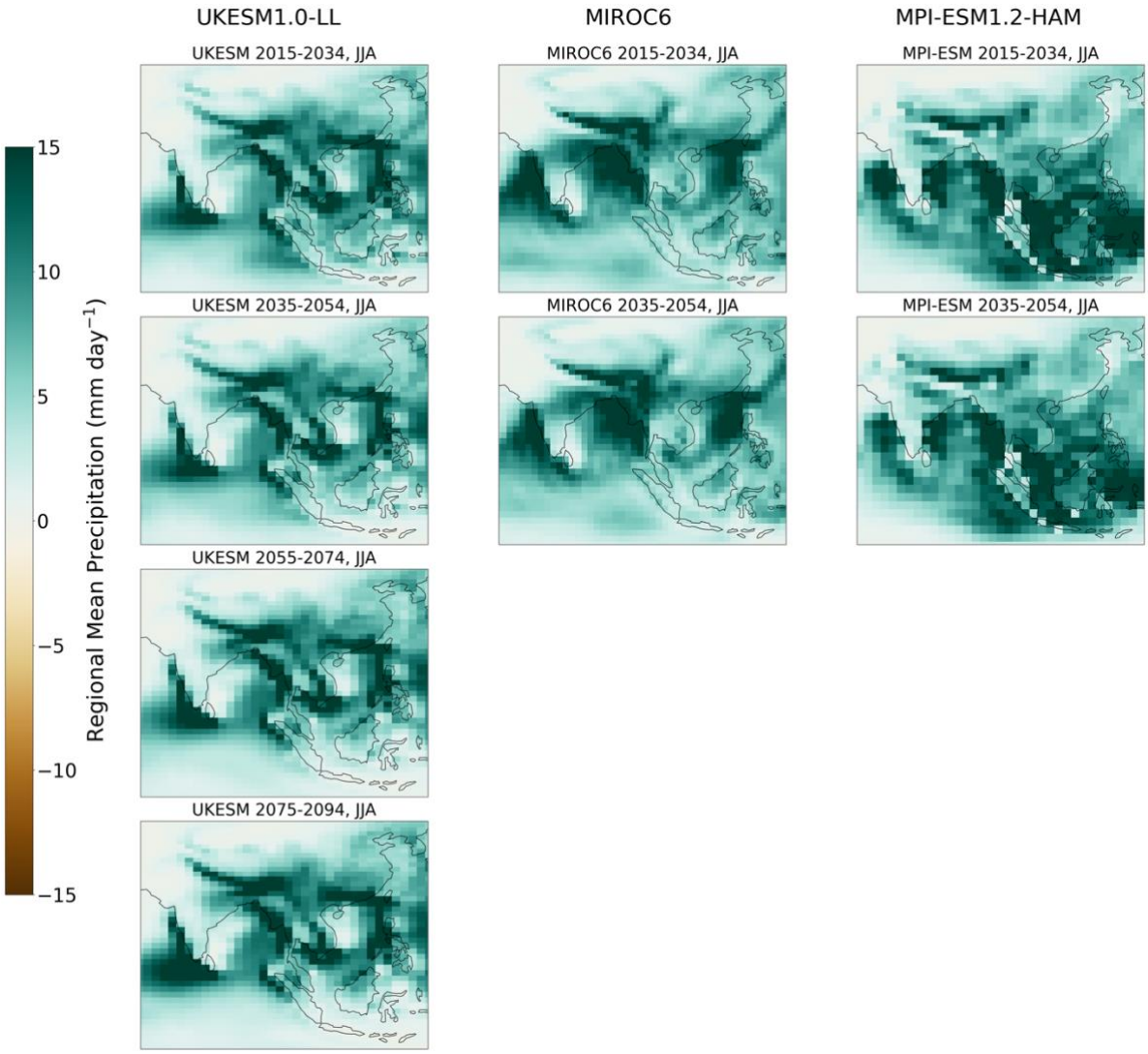

Figure 4.1: The ssp370 scenario regional mean JJA-mean absolute precipitation (mm day $^{-1}$) for 2015-2034 and 2035-2054 (additional 2055-2074 and 2075-2094 for UKESM). The region focuses on India and China, covering the geographical area that expands from 65˚E to 130˚E and from -10˚S to 40˚N. From the left column to the right, UKESM, MIROC and MPI-ESM.

Figure 4.1 presents the summer monsoon season's absolute precipitation for the ssp370 scenario in each model by regional mean JJA-mean. This plot explains how this season's expected average precipitation trends are distributed over South and East Asia, facilitating more straightforward comparisons for later.

The left, middle, and right columns display projections from UKESM, MIROC, and MPI-ESM, with each panel representing a 20-year mean. Most figures utilize the same layout for the rest of the results section.

There is consistency in expected precipitation patterns across models but with varying intensity levels. The anticipated precipitation remains concentrated across the Arabian Sea, Northern India, the Bay of Bengal, the Tibetan Plateau, and the South and East China Sea. It is important to note that no t-test was conducted as the data was directly plotted from the models.

4.1 Aerosol Absorption Optical Depth (AAOD) Response

The analysis of all the models indicates a global decrease in AAOD in response to rapid reductions in BC emissions (see Fig. 4.2), with UKESM and MPI-ESM exhibiting a comparatively stronger signal. Conversely, MIROC displays only minor indications of the same.

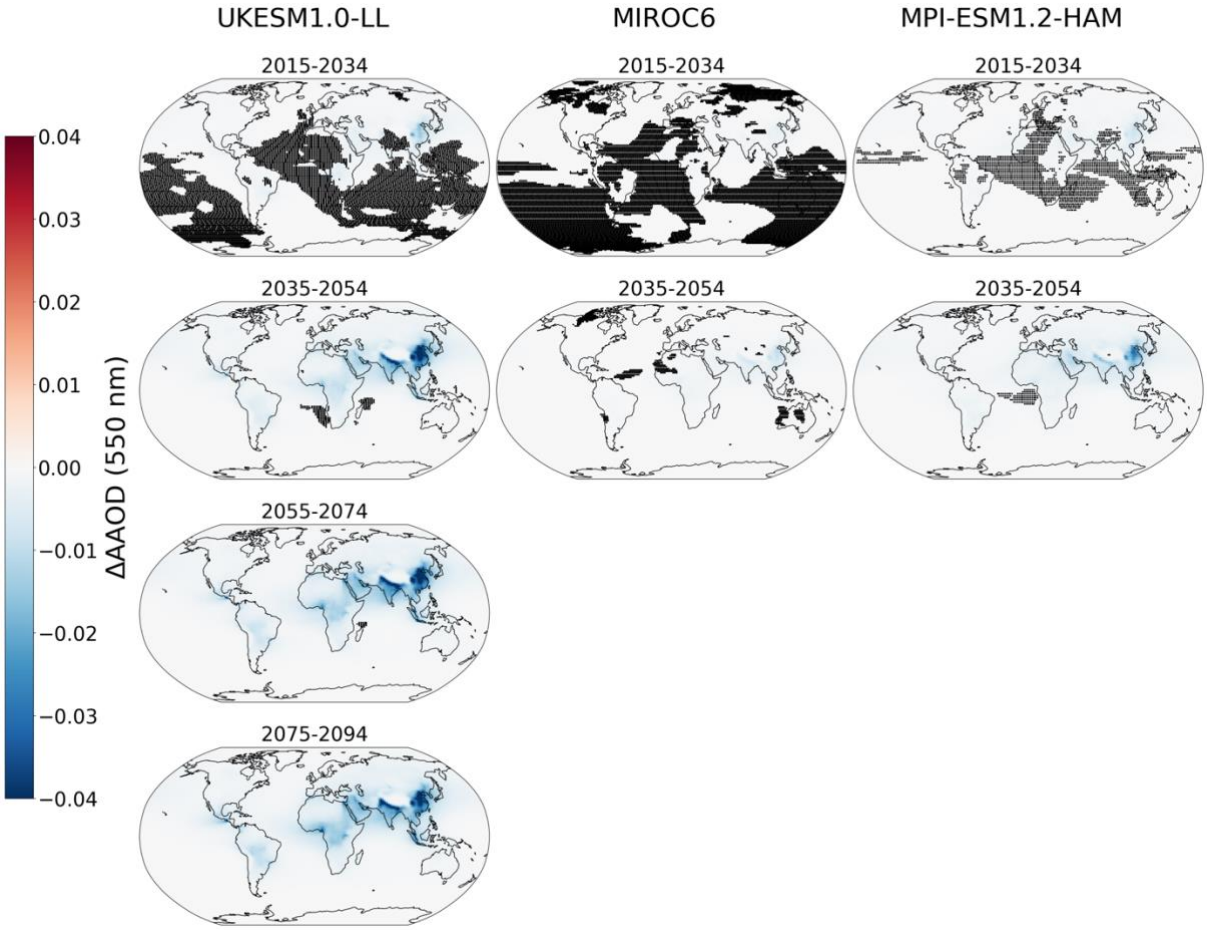

Figure 4.2: Global mean annual-mean AAOD anomalies at 550 nm for 2015-2034 and 2035-2054 (additional 2055-2074 and 2075-2094 for UKESM). From the left column to the right, UKESM, MIROC and MPI-ESM. Non-significant trends are highlighted.

All models' most significant AAOD anomalies are over Asia, particularly India and China (Fig. 4.2, 4.3). UKESM and MPI-ESM also show decreases in AAOD over the Sub-Saharan region in Africa.

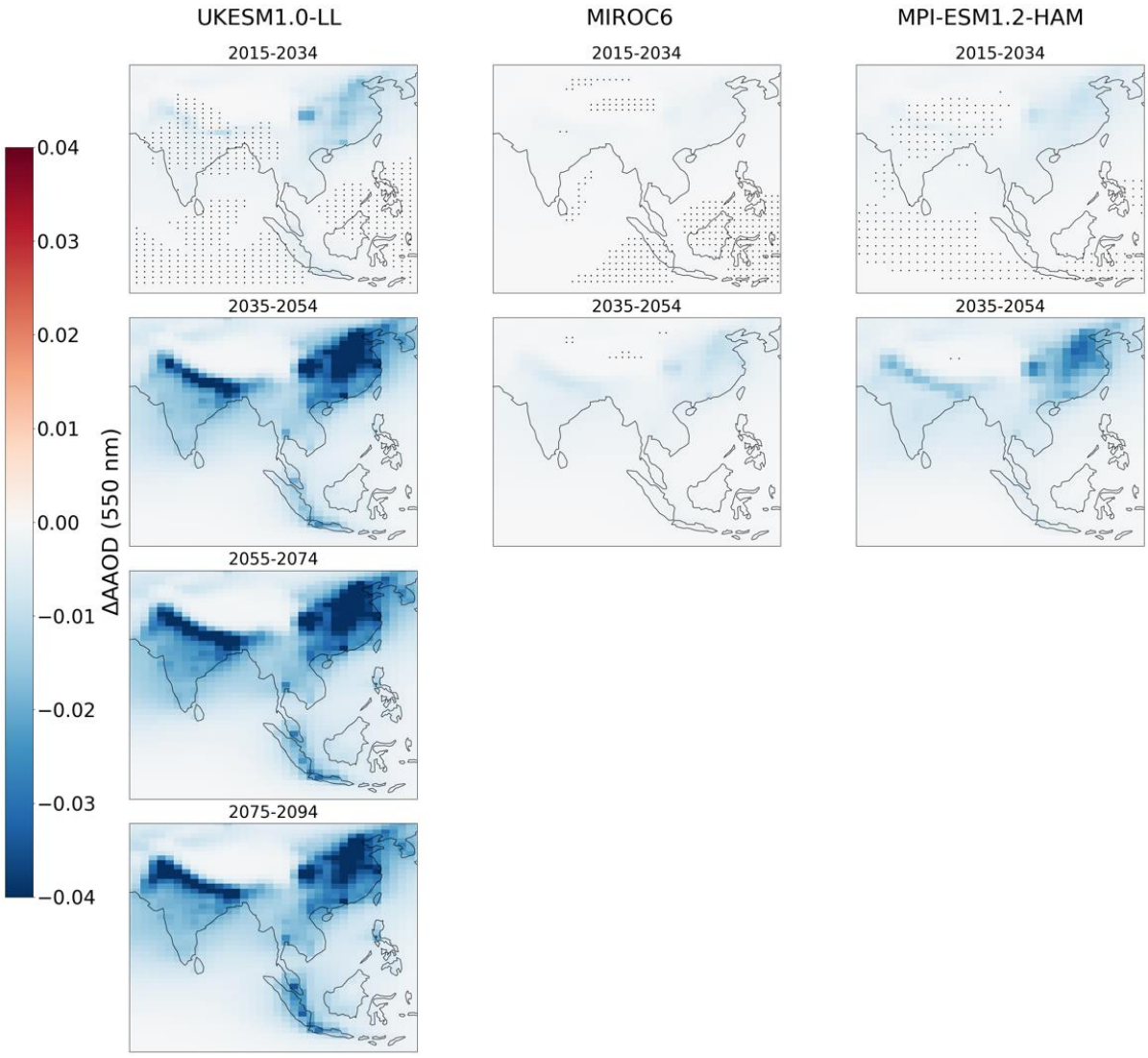

Figure 4.3: Regional mean annual-mean AAOD anomalies at 550nm for 2015-2034 and 2035-2054 (additional 2055-2074 and 2075-2094 for UKESM). From the left column to the right, UKESM, MIROC and MPI-ESM. Non-significant trends are highlighted.

A comparison of the regional mean for the models shows that it is evident that all three models concur on the decrease in AAOD within specific regions. Still, they differ on the magnitude of the change. Notably, the models indicate the reduction in Northern India and below the Tibetan Plateau, as well as Eastern China and around heavily populated and polluted cities such as New Delhi and Beijing.

The seasonal mean AAOD anomalies are shown in Figure 4.4, with the winter season (DJF) leading the most significant response for all models.

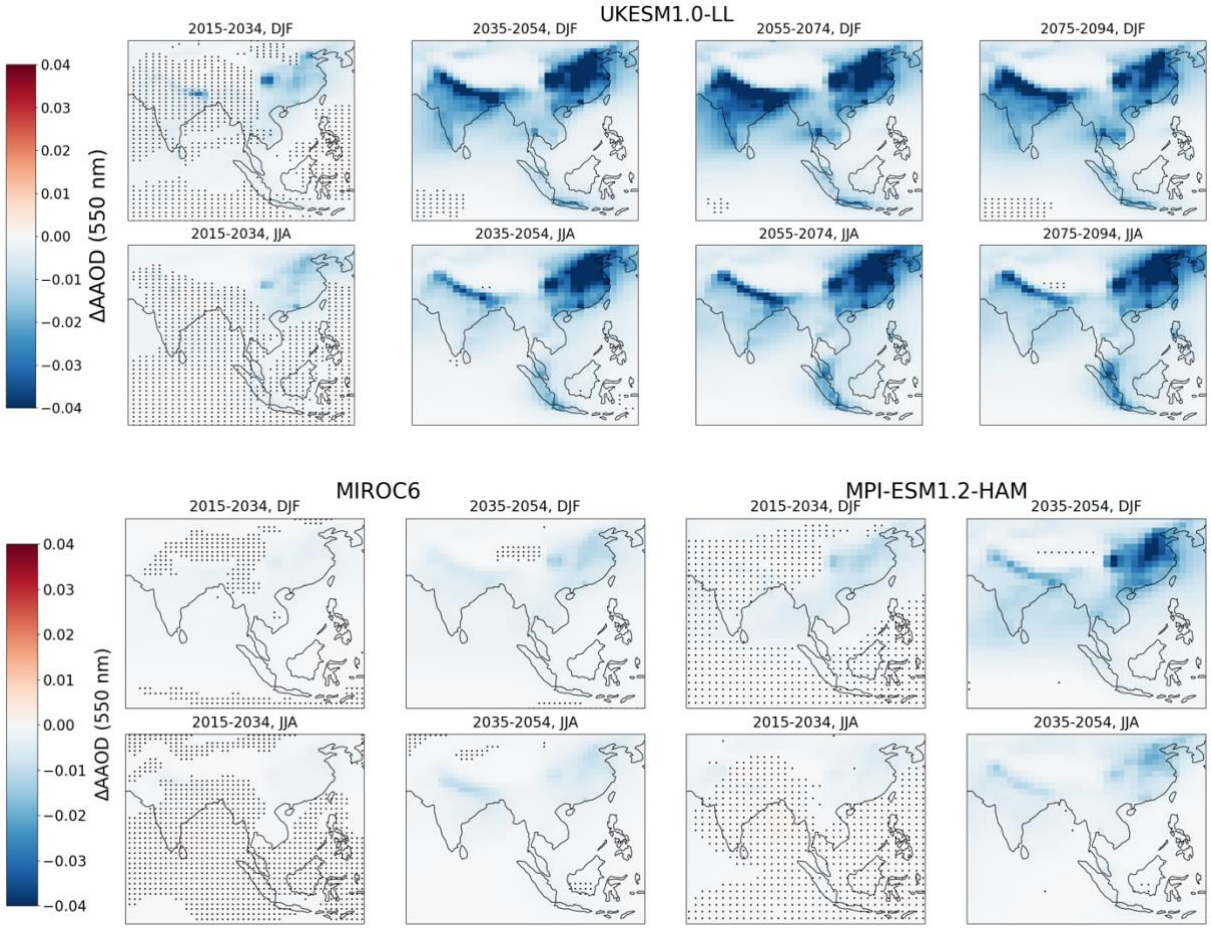

Figure 4.4: Seasonal mean AAOD anomalies at 550nm for 2015-2034 and 2035-2054 (additional 2055-2074 and 2075-2094 for UKESM). The first two rows represent UKESM results. The last two rows represent MIROC (left) and MPI-ESM (right) results. The rows represent seasons (DJF, JJA), and the columns represent corresponding intervals. Non-significant trends are highlighted.

4.2 Near-Surface Air Temperature (tas) Response

Figures 4.5 and 4.6 show the global mean and regional mean near-surface temperature anomalies in response to the AAOD changes presented in the previous section.

The models suggest that mitigating BC has a limited impact on global-mean near-surface air temperature evolution. Nevertheless, the observed effects include some regional and seasonal temperature responses.

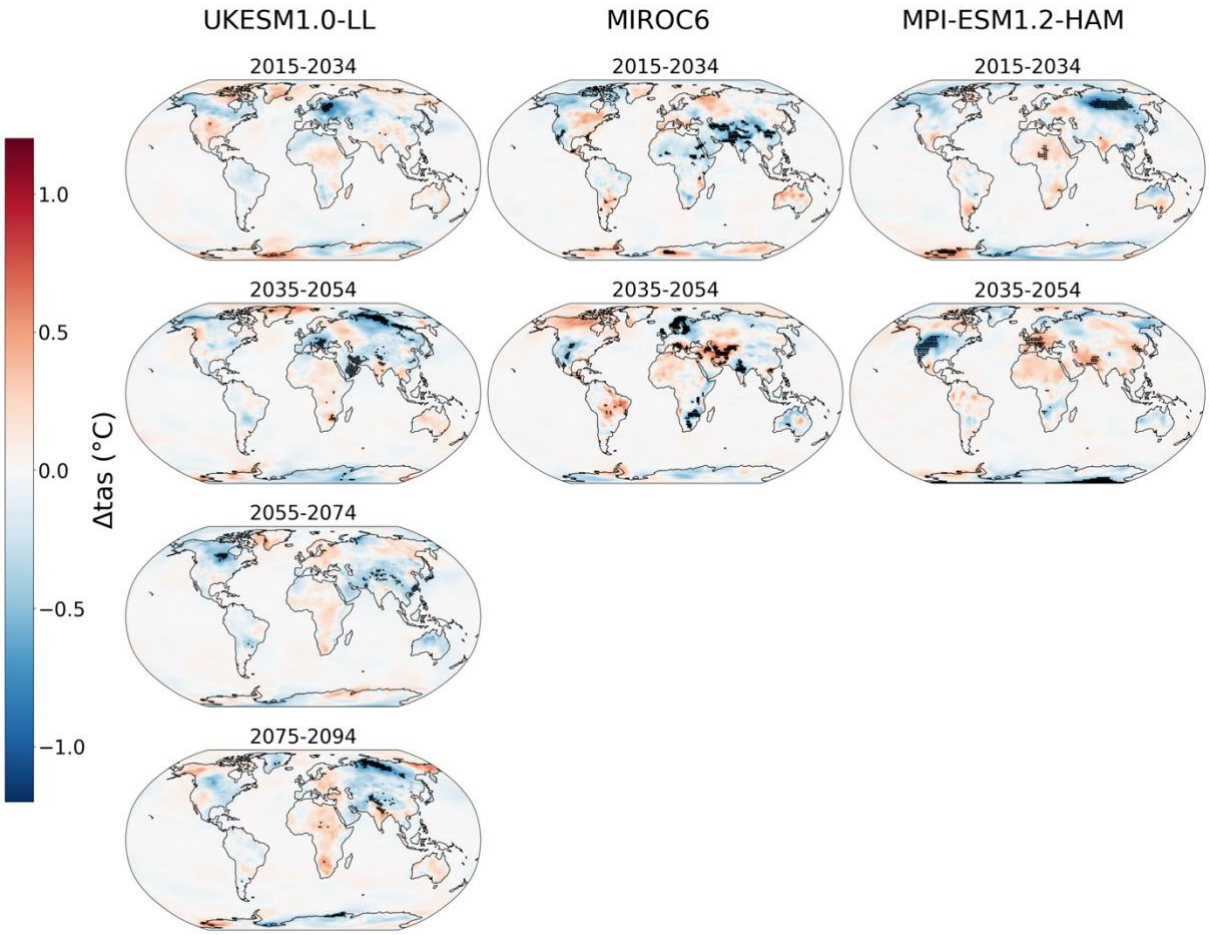

Figure 4.5: Global mean annual-mean tas anomalies for 2015-2034 and 2035-2054 (additional 2055-2074 and 2075-2094 for UKESM). From the left column to the right, UKESM, MIROC and MPI-ESM. Significant trends are highlighted.

The different models indicate varying patterns and magnitudes of regional mean temperature anomalies due to the mitigation of BC (Fig. 4.6). UKESM predicts significant warming over substantial areas in India and surrounding Beijing, while other regions of China, notably the Tibetan plateau and South China, experience a cooling effect. Meanwhile, MPI-ESM suggests a similar warming in India, with significant changes in the Northwest and a marked rise in temperature over Eastern China. MIROC, on the other hand, predicts a significant cooling trend over most areas in India and China during the first interval (2015-2034), followed by a warming over China and a further cooling in India in the next (2035-2054).

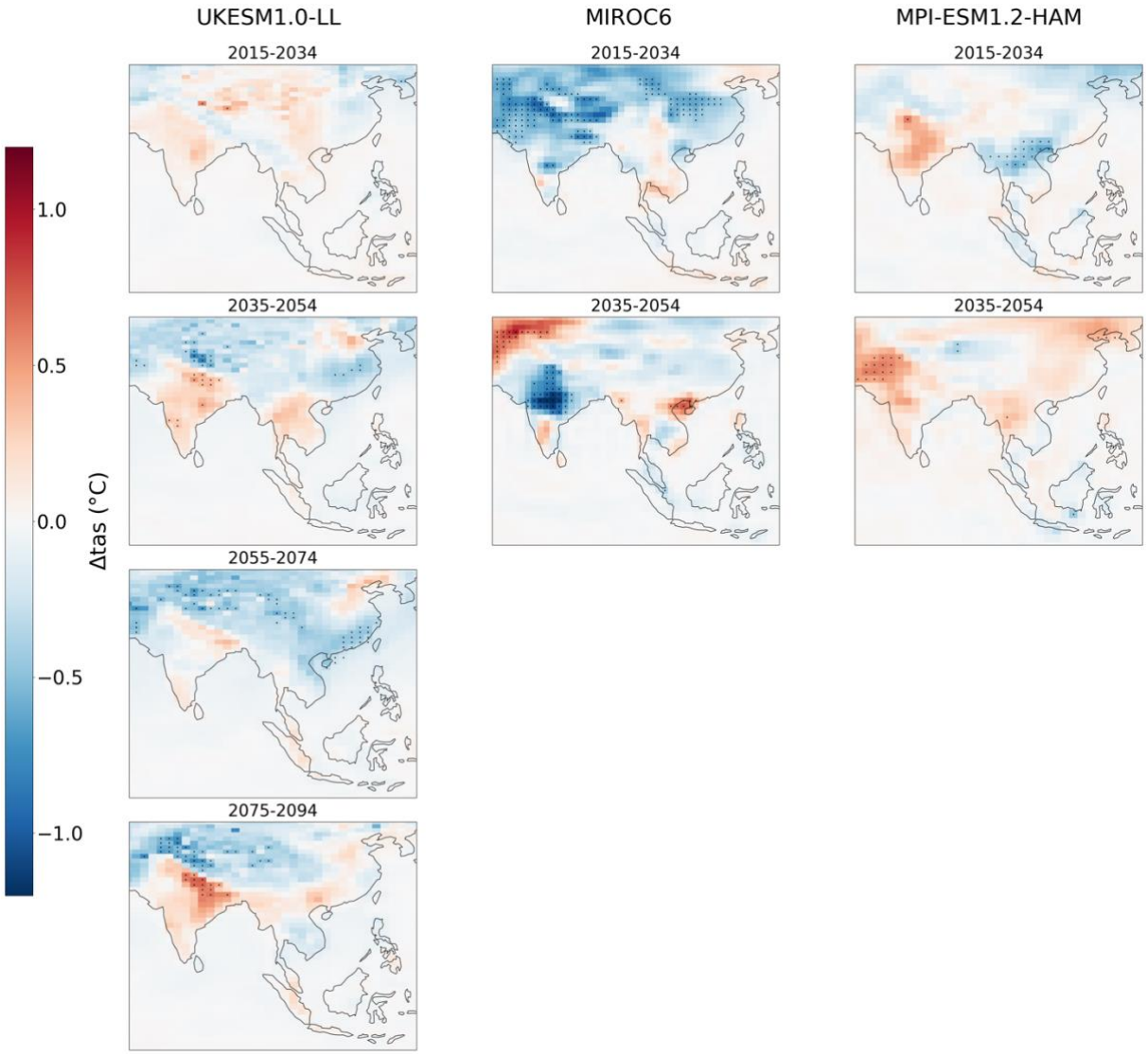

Figure 4.6: Regional mean annual-mean tas anomalies for the 2015-2034 and 2035-2054 (additional 2055-2074 and 2075-2094 for UKESM). From the left column to the right, UKESM, MIROC and MPI-ESM.

Seasonal variations have a noticeable impact on the results (see Fig. 4.7). According to UKESM, the winter season in the Tibetan plateau experiences a lot of noise. UKESM also projects a cooling in India and significantly Eastern China until 2074, followed by a warming in both regions by 2094. During the summer, there are significant patterns: cooling over the Tibetan plateau and Eastern China (except over Beijing, which remains relatively unchanged) and a steady temperature increase over India.

MIROC projects a significant cooling over China and Northern India in winter, followed by warming over most of China and Southern India by 2054. During the summer, MIROC predicts a significant cooling in the area around New Delhi and the Tibetan plateau, a slight warming around Beijing by 2054, followed by significant warming in the west Tibetan plateau, and cooling in most of India except the southern areas.

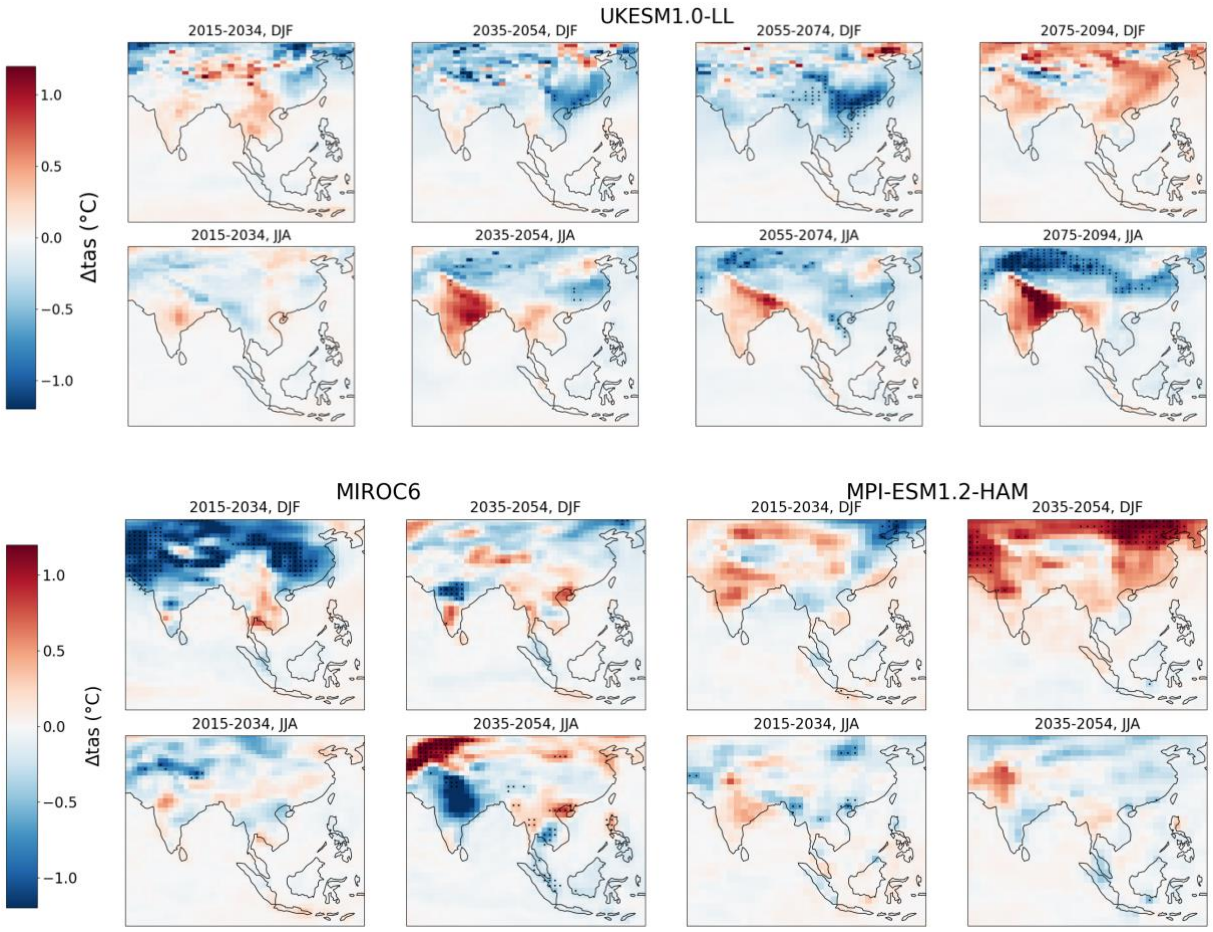

Figure 4.7: Seasonal mean tas anomalies for 2015-2034 and 2035-2054 (additional 2055-2074 and 2075-2094 for UKESM). The first two rows represent UKESM results. The last two rows represent MIROC (left) and MPI-ESM (right) results. The rows represent seasons (DJF, JJA), and the columns represent corresponding intervals.

MPI-ESM projects a cooling in East China by 2034, followed by a significant rise in temperature during the winter in West India, North China, and East China by 2054. Conversely, by 2054, a marked cooling is expected during the summer in India and China, apart from New Delhi's surrounding area.

4.3 Vertical Mass Flux (omega) Response

Figure 4.8 depicts the regional mean anomalies in vertical mass flux (omega) at a pressure level of 850 hPa in the South and East Asian regions as a response to reductions in BC emission. The anomaly is calculated by inverting the sign of omega values, making a positive value indicative of upward motion.

UKESM shows an anticipated increase in the mean omega over most of continental India and across the South and East China Seas, promoting ascending air. In contrast, UKESM projects a significant decrease in omega over Northern India, the Arabian Sea, the Bay of Bengal, and Eastern China, promoting decreased ascending air.

The projections from MIROC and MPI-ESM present somewhat mixed anomalies. Both models indicate an increase in omega over the Indian Ocean and Southern India, suggesting enhanced upward air currents. For China, these models produce a lot of noise and no noticeable significant trends.

As depicted in Figure 4.9, the seasonal analysis highlights notable variations in omega at 850 hPa across the different models and seasons. During the summer, UKESM exhibits trends like those observed in the regional mean plot but with a notable amplification of increased omega over the Indian Ocean. Conversely, UKESM projects a significant decrease in omega over the coastal areas of India, the Bay of Bengal, and Eastern China during the winter season by 2094.

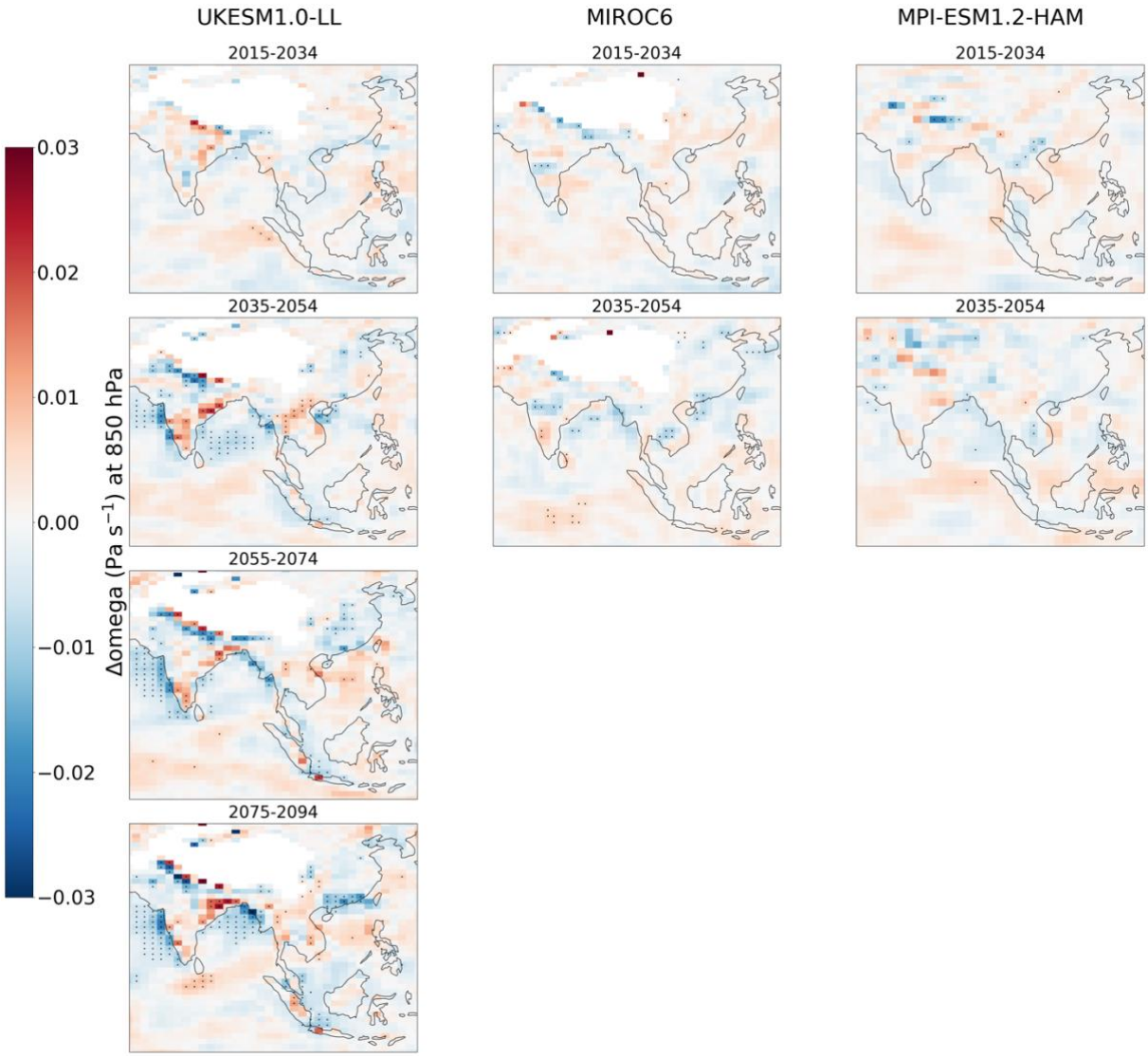

Figure 4.8: Regional mean annual-mean omega anomalies (Pa s^{-1}) measured at 850 hPa for 2015-2034 and 2035-2054 (additional 2055-2074 and 2075-2094 for UKESM). From the left column to the right, UKESM, MIROC and MPI-ESM.

MIROC and MPI-ESM show amplified seasonal patterns. Both models indicate a rising trend in omega over Northern and Southeast India for the summer season. The winter projections from MPI-ESM are characterized by considerable variability but tend to exhibit declining omega over continental India and China. MIROC, on the other hand, projects a significant pattern of decreasing omega in Northern India and Eastern China by 2054 as a response to mitigating BC emissions.

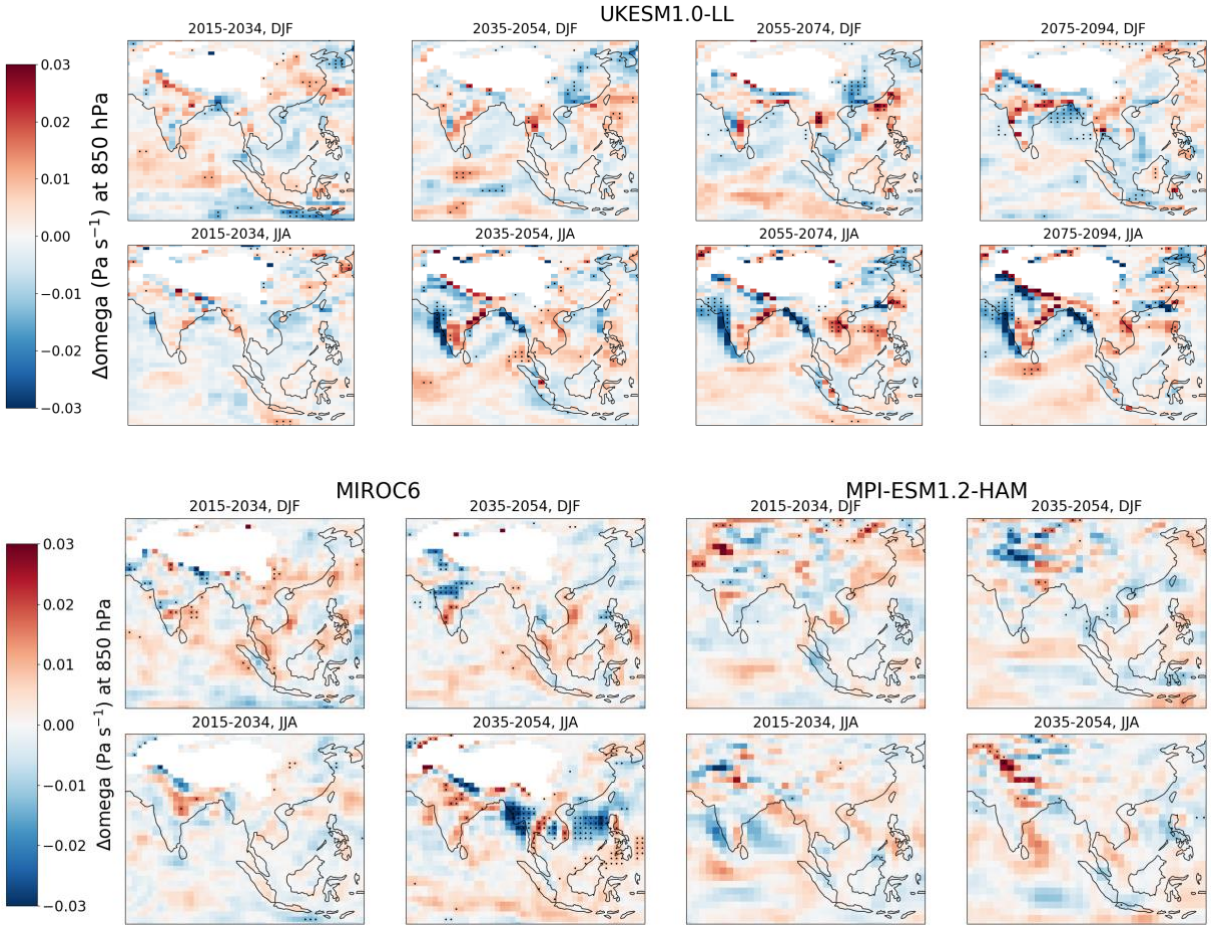

Figure 4.9: Seasonal mean omega anomalies (Pa s^{-1}) measured at 850 hPa for 2015-2034 and 2035-2054 (additional 2055-2074 and 2075-2094 for UKESM). The first two rows represent UKESM results. The last two rows represent MIROC (left) and MPI-ESM (right) results. The rows represent seasons (DJF, JJA), and the columns represent corresponding intervals.

A seasonal simulation is also conducted at a pressure level of 250 hPa (Fig. 4.10). According to the simulation, by 2054, UKESM projects decreased omega over India, while MIROC suggests increased omega higher in the atmosphere. MPI-ESM predicts similar results to those at 850 hPa.

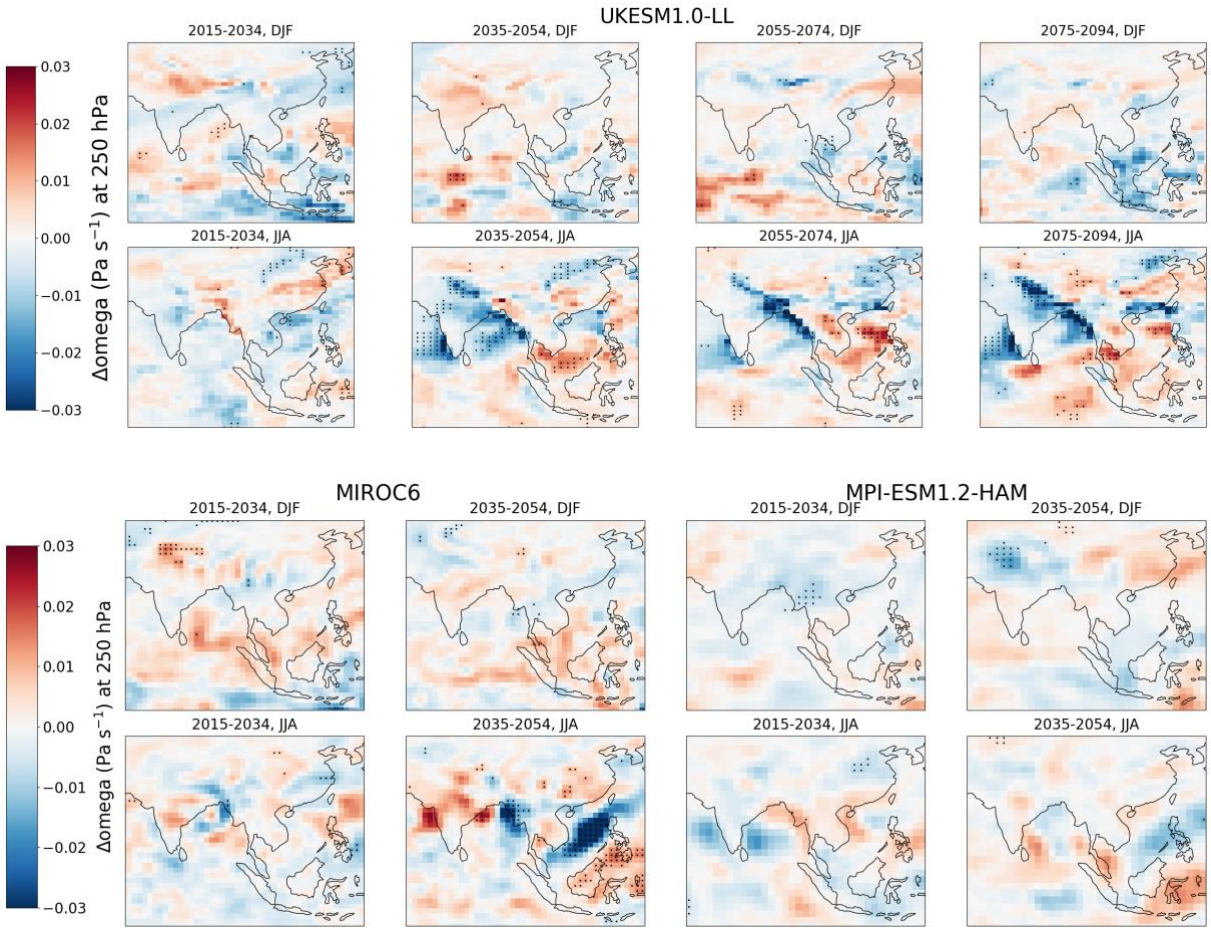

Figure 4.10: Seasonal mean omega anomalies (Pa s^{-1}) measured at 250 hPa for 2015-2034 and 2035-2054 (additional 2055-2074 and 2075-2094 for UKESM). The first two rows represent UKESM results. The last two rows represent MIROC (left) and MPI-ESM (right) results. The rows represent seasons (DJF, JJA), and the columns represent corresponding intervals.

4.4 Vertical Air Temperature (ta) Response

Figures 4.11 and 4.12 are curtain plots that show the mean vertical air temperature (ta) anomalies in the East and West Asia region as a response to a rapid reduction in BC emissions. Figure 4.11 covers the latitude of India and the Indochinese Peninsula, while Figure 4.12 includes the area further above India, including the Tibetan Plateau and China. The left, middle, and right columns display projections from UKESM, MIROC, and MPI-ESM, with each panel representing a 20-year mean. Each subplot's x- and y-axis represent longitude and pressure level (Pa).

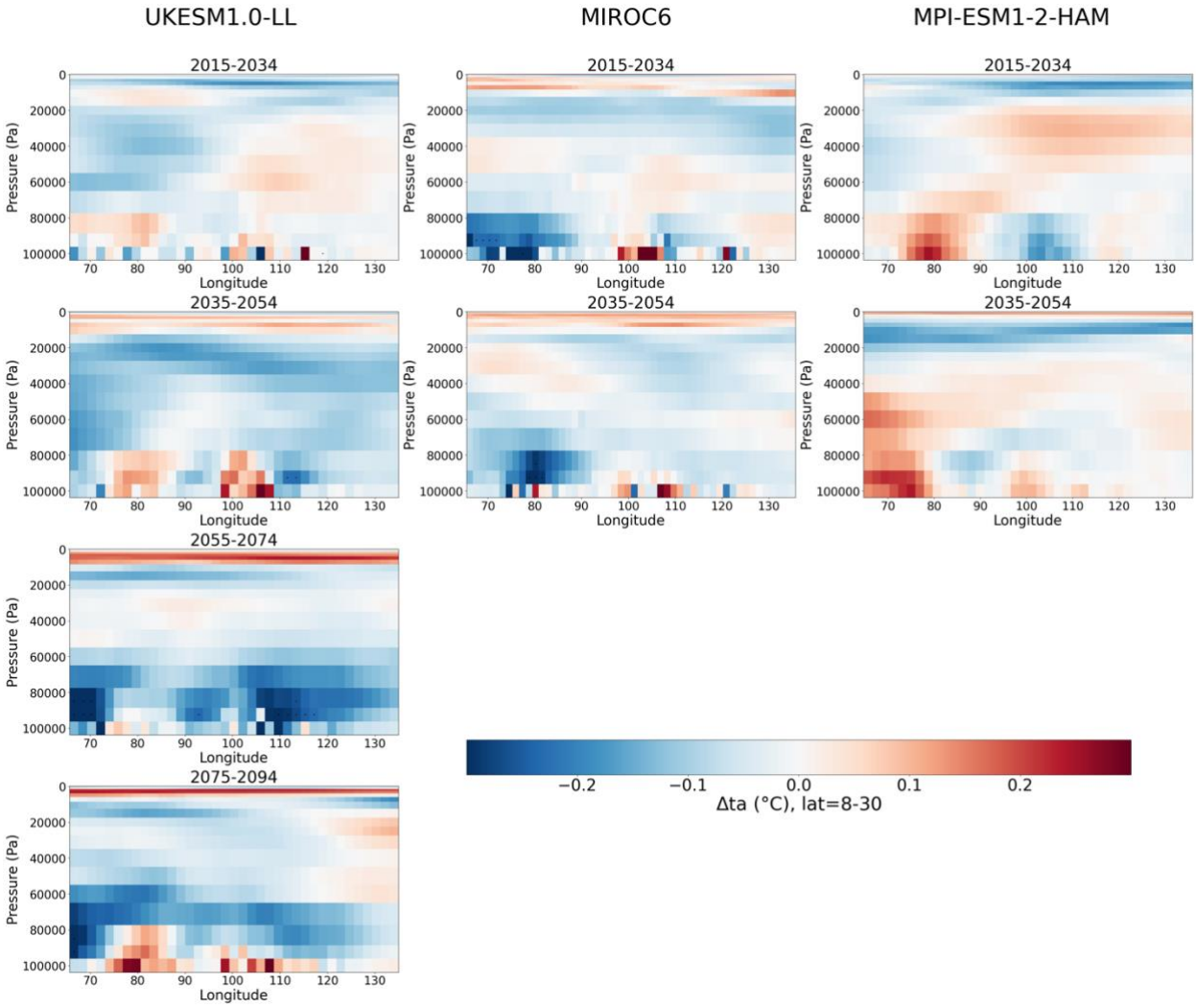

Figure 4.11: Regional mean annual-mean ta anomalies (°C) for pressure levels 0 to 100000 Pa in the atmosphere. Latitude and longitude are sliced to cover 8-30 °N and 65-135 °E, respectively. The intervals cover 2015-2034 and 2035-2054 (additional 2055-2074 and 2075-2094 for UKESM). From the left column to the right, UKESM, MIROC, and MPI-ESM.

The longitudes covering India (approximately 68-85°) are projected to experience increased surface warming and further tropospheric cooling by UKESM. MPI-ESM also indicates increased surface warming by 2034, followed by increased tropospheric temperatures. On the other hand, MIROC projects mixed responses but generally decreased surface temperatures that continue higher in the troposphere. All models agree on the increased stratospheric heating.

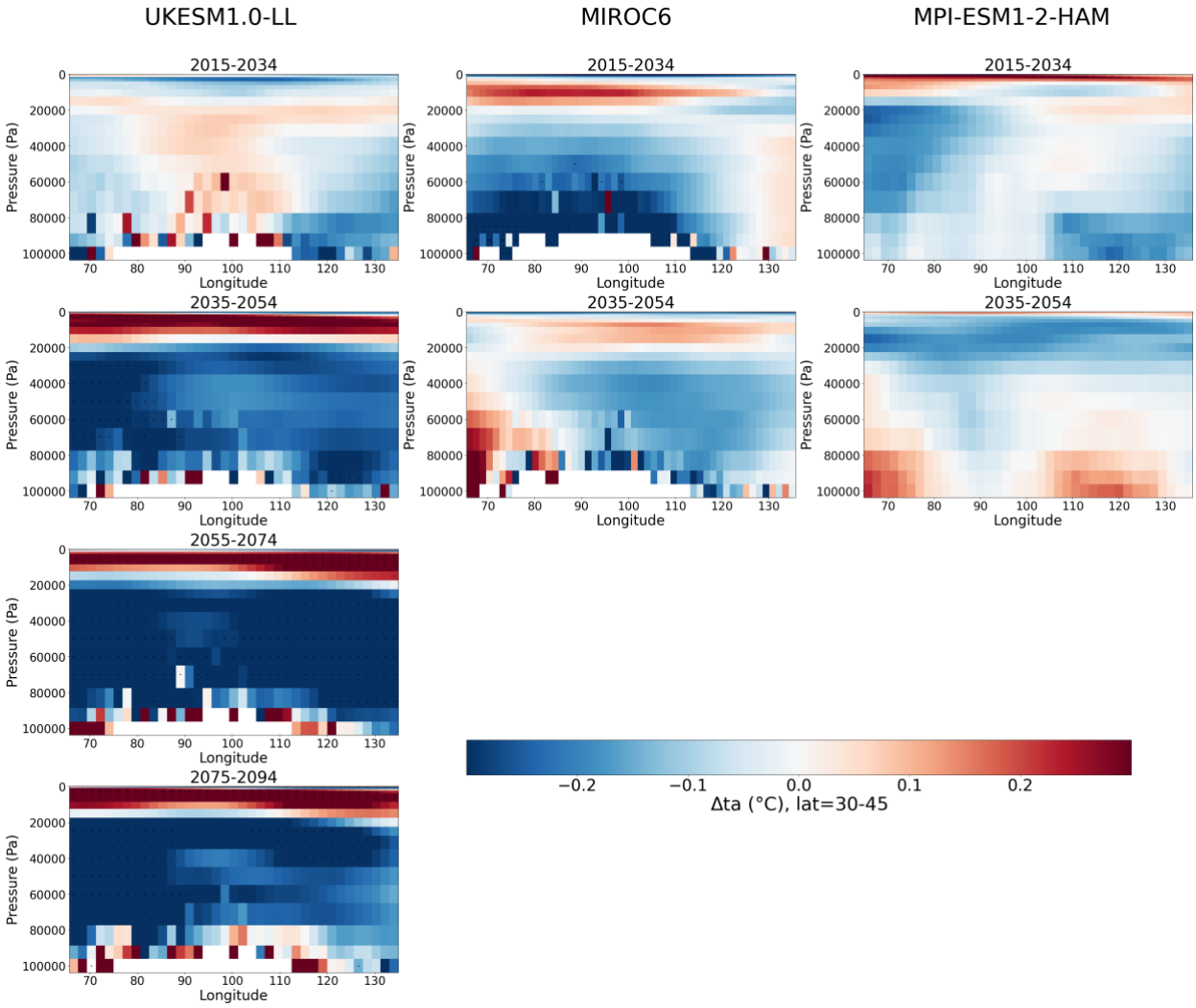

Figure 4.12: Regional mean annual-mean ta anomalies (°C) for pressure levels 0 to 100000 Pa in the atmosphere. Latitude and longitude are sliced to cover 30-45 °N and 65-135 °E, respectively, to cover the region, including China. The intervals cover 2015-2034 and 2035-2054 (additional 2055-2074 and 2075-2094 for UKESM). From the left column to the right, UKESM, MIROC, and MPI-ESM.

The models suggest that the latitudes covering the Tibetan Plateau and China have more decisive responses to reductions in BC emissions. UKESM anticipates an increase in surface temperatures over the longitudes of the Tibetan Plateau and Beijing (approximately 115-120°), succeeded by enhanced cooling in the troposphere and heating in the stratosphere by 2074. MIROC displays comparable patterns, apart from projecting decreased surface temperatures. Conversely, MPI-ESM indicates an initial decrease in surface and tropospheric temperatures, followed by increased surface temperatures over East and West China and further troposphere cooling by 2054.

4.5 Precipitation (pr) Response

Identifying consistent global precipitation patterns in response to reduced BC emissions is challenging. However, we can observe those near the Equator and the typical intertropical convergence zone (ITCZ) location (see Fig. 4.13).

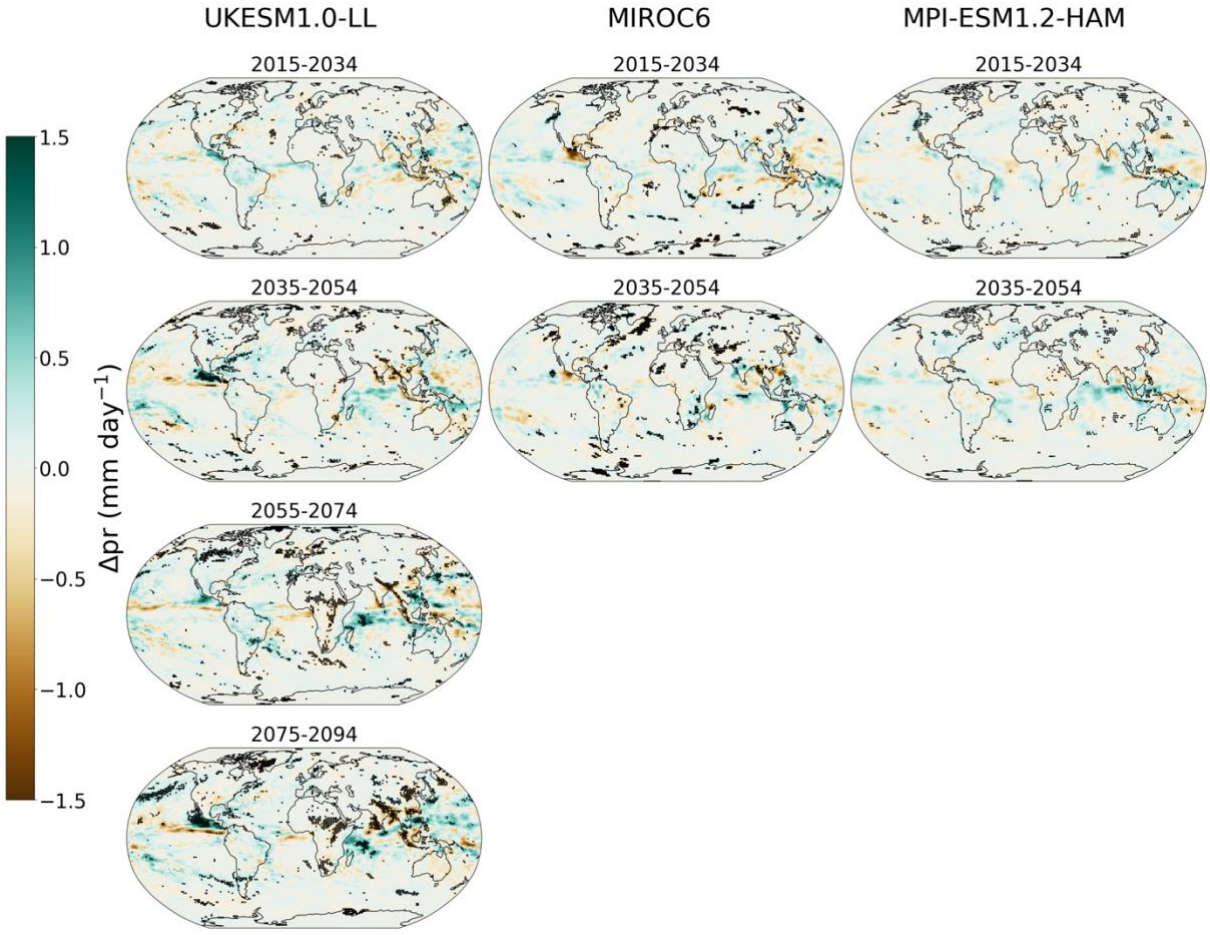

Figure 4.13: Global mean annual-mean pr anomalies (mm day^{-1}) for 2015-2034 and 2035-2054 (additional 2055-2074 and 2075-2094 for UKESM). From the left column to the right, UKESM, MIROC and MPI-ESM. Significant trends are highlighted.

Precipitation changes across the South and East Asian region show noteworthy trends (see Fig. 4.14). UKESM shows regional mean precipitation is projected to decrease for India and China. By the southern slope of the Tibetan Plateau, over the Arabian Sea, and the Bay of Bengal, UKESM predicts significant trends of declining precipitation.

MIROC anticipates increased precipitation over India by 2054, little change over China, and decreased precipitation over the South China Sea. MPI-ESM indicates decreased precipitation over continental India and China. There is an observed increase in precipitation over the Indian Ocean for all models.

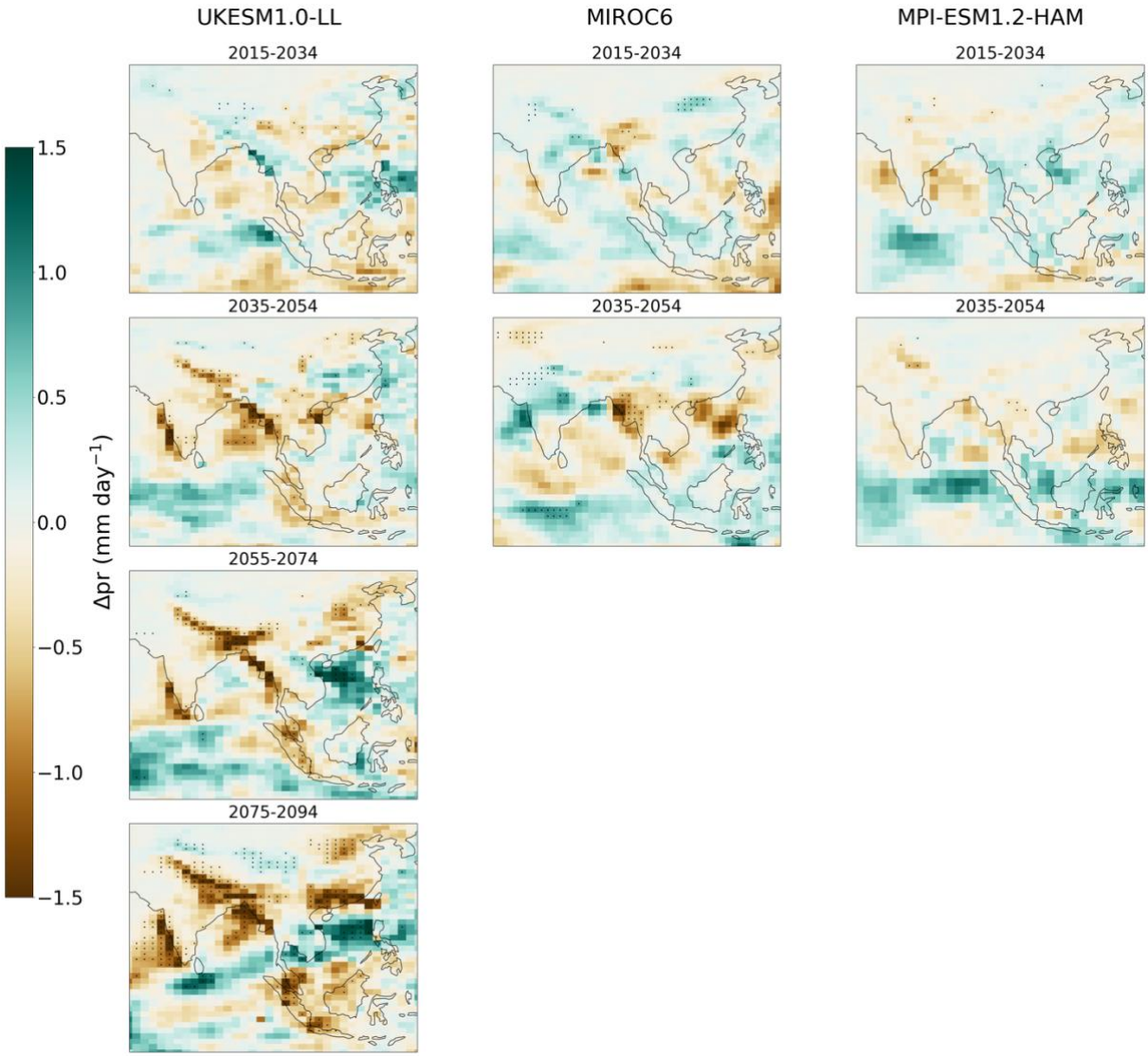

Figure 4.14: Regional mean annual-mean pr anomalies (mm day^{-1}) for 2015-2034 and 2035-2054 (additional 2055-2074 and 2075-2094 for UKESM). From the left column to the right, UKESM, MIROC and MPI-ESM.

Regarding the seasonal mean precipitation simulations, all climate models concur on drier winter seasons in the region by 2054 (see Fig. 4.15). UKESM anticipates mainly decreases in precipitation over land, while MIROC and MPI-ESM predict the opposite. UKESM projects robust declines in precipitation in the summer season, especially over North India, Northeast China, the Arabian Sea, and the Bay of Bengal in the coming decades. However, Southeast China and the Tibetan Plateau exhibit increased precipitation projections. MIROC projects significantly increased precipitation over India and eastern China by 2054 and a robust decrease over the South and East China Sea. MPI-ESM initially projects similar results to those from UKESM, followed by results more like those from MIROC by 2054.

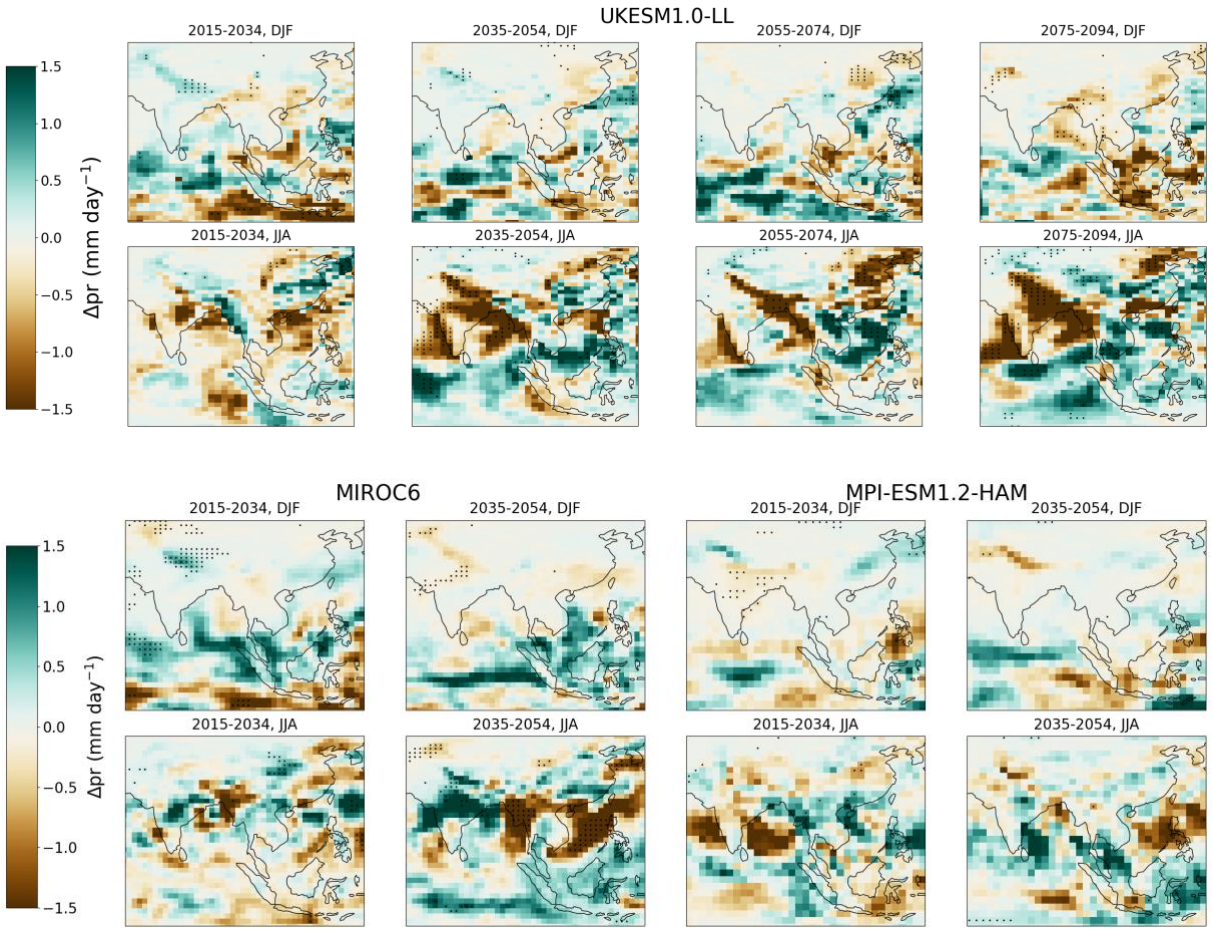

Figure 4.15: Seasonal mean pr anomalies (mm day^{-1}) for 2015-2034 and 2035-2054 (additional 2055-2074 and 2075-2094 for UKESM). The first two rows represent UKESM results. The last two rows represent MIROC (left) and MPI-ESM (right) results. The rows represent seasons (DJF, JJA), and the columns represent corresponding intervals.

The examination of seasonal mean precipitation can be facilitated using a percent-change plot (see Fig. 4.16). The models suggest that winter precipitation will decrease by 2054/2094 due to reductions in BC emissions. While UKESM anticipates a significant reduction, MIROC and MPI-ESM indicate a rise in summer monsoon precipitation, consistent with the absolute precipitation projections (Fig. 4.15).

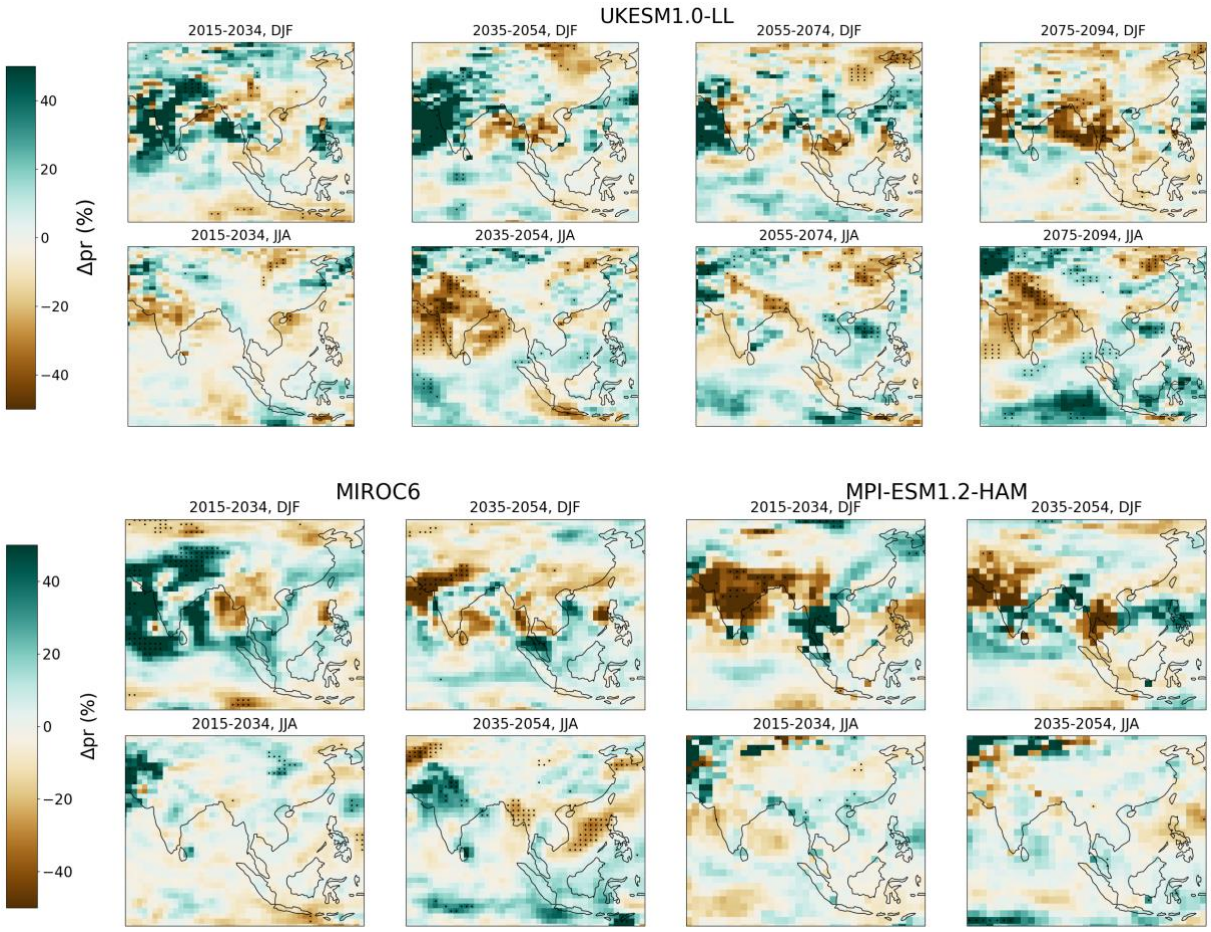

Figure 4.16: Seasonal mean pr anomalies (%-change) for 2015-2034 and 2035-2054 (additional 2055-2074 and 2075-2094 for UKESM). The first two rows represent UKESM results. The last two rows represent MIROC (left) and MPI-ESM (right) results. The rows represent seasons (DJF, JJA), and the columns represent corresponding intervals.

5 Discussion

Over the past decades, South China has encountered increased summer floods, while North China has faced more frequent droughts. Meanwhile, China and India have undergone moderate surface cooling, contrasting with the warming trend observed in the rest of the world (Menon et al., 2002). This section delivers an overview of our results and establishes a connection between the findings and climate patterns witnessed throughout Asia. Subsequently, we will delve into the significance of these discoveries, including their impact on the Asian monsoon, limitations, uncertainties, and avenues for future research.

5.1 Summary of Global and Regional Responses

All three models - UKESM, MIROC, and MPI-ESM - project global decreases in AAOD in response to reduced BC emissions. The most significant changes will occur in South and East Asia (see Fig. 4.2, 4.3) and are most noticeable in the "aerosol hotspot" areas around New Delhi and Beijing, which is consistent with their status as significant sources of aerosols and their precursors (Ramachandran et al., 2022). The strong responses align with our experimental setup, which contrasts the ssp370 scenario, featuring the highest level of SLCFs and weak levels of air quality control measures (Fig. 2.6), with the ssp370-lowBC scenario, which is perturbed by strong levels of air quality control measures for BC.

The mitigation of BC emissions has a limited global impact on the near-surface temperature (Fig. 4.5), which supports the findings of Stjern et al. (2017). Fig. 4.6 shows that by 2054, India and China will experience warming and cooling trends, likely due to model internal variability causing arbitrary patterns. Little response on near-surface temperature is expected, as our simulation setup uses fSSTs.

Identifying trends of change in regional mean vertical mass flux across Asia in response to reduced BC emissions poses a challenge due to the somewhat mixed signals from MIROC and MPI-ESM (Fig. 4.18). However, the projections presented by UKESM are significant and indicate decreased ascending air over Northern India, the oceans surrounding India, and Eastern China, while increased ascending air is projected over most of continental India by

2054. Decreased ascending air implies increased atmospheric pressure and reduced convective activity, promoting atmospheric stabilization. Increased ascending air, conversely, suggests a more dynamic and unstable atmosphere.

Mitigation of BC in the atmosphere is expected to induce surface warming and weaken atmospheric radiative heating (Takemura & Suzuki, 2019). Figures 4.11 and 4.12 depict that the models mostly agree with this anticipation. All models project decreasing temperatures in the troposphere and a rise in temperature in the stratosphere - with UKESM displaying a more marked response over the Tibetan Plateau (Fig. 4.12). Conversely, MPI-ESM suggests surface temperature increases and tropospheric heating for India and Eastern China, while the upper troposphere has a cooling effect.

UKESMs' vertical temperature change over India is worth noticing (Fig. 4.11). Projections indicate that temperatures increase up to 800 hPa by 2054, affecting the planetary boundary layer, which is the most turbulent region of the atmosphere. The observation is that removing BC from the atmosphere increases surface warming, which consequently spreads upwards to the lower atmospheric layers. The projections from UKESM and MIROC generally enhance atmospheric temperature patterns (see Fig. 2.2). Meanwhile, MPI-ESM presents somewhat contradictory results. This may be attributed to the lower MPI-ESM model resolution, the number of vertical levels, and its simplified treatment of BC relative to the other models.

Global precipitation patterns remain mostly unchanged except for regions near the equator and ITCZ, where the response varies (Fig. 4.13). These regions tend to be responsive to climate change (Byrne et al., 2018). Reducing BC emissions is anticipated to increase regional mean precipitation, as previous research has found that BC has a drying effect on precipitation (e.g., Samset et al. (2016)). Nevertheless, the regional response varies among the models (Fig. 4.14). UKESM projects significantly reduced precipitation over most of India and China, whereas MIROC indicates increased precipitation over India. MPI-ESM suggests minimal overall change. All models concur on responses characterized by a dipole over the Indian Ocean, with increased precipitation south of the Equator and decreased north of it.

5.2 Seasonal Variations Influencing Responses

Based on Figure 4.4, it is evident that the changes in AAOD vary across different seasons, with winter displaying the most robust response to a reduction in BC emissions. This can be attributed to several factors related to atmospheric conditions, emission patterns, and regional climate dynamics. During winter, the atmosphere tends to be more stable with less vertical mixing, and the boundary layer is lowered due to cooler temperatures, leading to the accumulation of aerosols (Ansari & Ramachandran, 2023). In addition, winter presumably experiences more emissions due to increased domestic heating and biomass burning, and lower precipitation levels reduce the rate of BC wet deposition. The Tibetan Plateau's topographical features, including temperature inversions, impact atmospheric circulation, trapping pollutants and limiting their dispersion, resulting in heightened AAOD for this area during winter (Zhao et al., 2019).

Conversely, summer experiences higher temperatures, leading to unstable atmospheric conditions, a higher planetary boundary layer, and vertical mixing and dispersion are more common. The ASM circulation also influences the summer climate in the region, bringing changes in wind patterns, humidity, and precipitation levels, which impact BC distribution and lifetime due to wet deposition (Ramachandran & Rupakheti, 2022). These factors, alone or in combination, could contribute to the observed seasonal variations in AAOD anomalies.

The seasonal mean near-surface temperature response to a reduction in BC emissions varies between models and locations (see Fig. 4.7). The projections are characterized by significant patterns for UKESM, especially during the summer. MIROC and MPI-ESM, on the other hand, have contradictory responses. The models mostly agree on increased surface temperatures over India by 2054 for the winter season. However, the models notably disagree on whether the temperature increases or decreases over East China.

According to previous research, it has been found that BC does not have a significant impact on near-surface air temperatures (e.g., Stjern et al. (2017)). This is due to the climate system's rapid adjustment and an increase in low-level clouds due to fSSTs. However, reducing BC emissions is expected to result in less atmospheric heating and decrease low-level clouds while increasing middle- and high-level clouds (Takemura & Suzuki, 2019). These combined effects likely cause a gradual change in near-surface air temperatures rather than an

immediate or marked temperature increase. This is likely the case for UKESM's projection (Fig. 4.7).

As mentioned, the atmosphere tends to be more stable in the winter, resulting in a gradual change in surface temperature. On the other hand, the summer season is characterized by instability, and the surface temperature shows early signs of rapid changes. The ASM also contributes towards aerosol removal during the summer, which may allow more shortwave radiation to pass through to the surface, further contributing to the surface warming patterns over India. But this does not explain the surface cooling experienced in China. Hence, we attribute it to internal variability.

The seasonal mean vertical mass flux anomalies highlight increased and decreased ascending air variations for the different pressure levels in response to reduced BC emissions (see Fig 4.9, 4.10). Nonetheless, certain continental variations remain discernible. By 2054, the models predict primarily decreased ascending air at the 850 hPa pressure level during winter, particularly in China, likely due to the atmospheric stability typical for this time of year. UKESM and MIROC models exhibit dipole anomalies in India, with stabler atmospheric conditions in the north and less stable in the south. For the 250 hPa pressure level, both models project unstable atmospheric conditions, although they are not statistically significant.

Regarding the summer season, UKESM and MIROC project large variations in the patterns for both pressure levels by 2054, which is expected with extra turbulence. There is a clear pattern of decreased ascending air at 850 hPa over the Indian coast of the Arabian and Laccadive Sea for UKESM. On the other hand, the East Coast of India experiences unstable atmospheric conditions, which is also the case for MIROC. Higher up in the atmosphere, at 250 hPa, UKESM projects mainly stabilization over the same areas, while MIROC expects an unstable atmosphere. The Indian Ocean is generally characterized by less stable atmospheric conditions for all models. MPI-ESM projects overall vague responses, which can be attributed to MPI-ESM's model resolution and number of vertical levels.

Upon examination of the seasonal mean precipitation plots, it is apparent that the models exhibit varying responses to mitigating BC emissions (see Fig. 4.15). The absolute precipitation change projection during the winter monsoon remains largely unaffected across

continental India and China for all models. Nevertheless, the models suggest a slight decrease in precipitation in Northern India and Eastern China by 2054. As for the summer season, the response varies between models. UKESM projects a decrease over most of India and East China, MPI-ESM initially exhibits a decrease followed by increases in precipitation, and MIROC projects precipitation increases over the exact locations. A percentage change projection is also generated for comparative analysis (Fig. 4.16). Nevertheless, it is noteworthy that such projections may be prone to misinterpretation as the areas and seasons that typically experience low precipitation levels can show significant deviations. Precipitation and the ASM are discussed further in section 5.4.

5.3 Interconnections Among the Climate Variables

This section examines the response of climate variables in each model to the reduction in BC emissions while also analyzing the interconnections between the variables.

Reduced BC emissions may trigger a feedback loop that leads to a more dynamic atmosphere with enhanced cloud formation, contrary to the expected outcome of increased BC. However, the climate in South and East Asia is intricate due to other aerosols, monsoon systems, and diverse topography, further complicating the matter. Moreover, the response of climate models to these elements may vary, causing model disagreement.

UKESM projections show robust decreases in AAOD in North India, the Tibetan Plateau, and East China (Fig. 4.3, 4.4). In response, the troposphere cools over these areas (Fig. 4.11, 4.12), and the surface temperature increases in North India and Northeast China. Conversely, it decreases over the Tibetan Plateau and Southeast China (Fig. 4.6, 4.7). Removing BC results in a marked tropospheric cooling over the Tibetan Plateau and Southeast China (Fig. 4.12). This leads to unstable atmospheric conditions with increased convective activity (Fig. 4.8-4.10), which may explain the increased precipitation (Fig. 4.14, 4.15).

The surface warming over India and Northeast China is expected to cause atmospheric instability. Nevertheless, UKESM projects a decrease in precipitation in these areas (Fig. 4.14, 4.15). We attribute this to the convective activity at 250 hPa (Fig. 4.10), depicting overall stabilization for both areas. The patterns of stabilizing atmospheric conditions are observed over the Arabian Sea and the Bay of Bengal. These are the areas where precipitation usually

occurs (Fig. 4.1). These findings indicate that for UKESM, convective activity primarily controls the precipitation response to a reduction of BC.

MIROC, on the other hand, projects increased precipitation over Northern India and a slight response in China (Fig. 4.14, 4.15). The difference between MIROC and UKESM is the level of the decrease in AAOD, where MIROC shows weaker responses (Fig. 4.3, 4.4). This indicates that MIROC may be less sensitive to BC reductions. Consequently, the projections show surface temperature decreases (Fig. 4.6, 4.7) and increased temperatures higher in the atmosphere (Fig. 4.11, 4.12), leading to convective activity and an unstable atmosphere over Northern India (Fig. 4.8-4.10).

MPI-ESM projects little overall change in precipitation but indicates slightly increased levels over India and China (Fig. 4.14, 4.15). It projects robust decreases in AAOD over North India and East China (Fig. 4.3, 4.4). As a response, increased surface warming (Fig. 4.6, 4.7) and planetary boundary layer warming are observed over both areas (Fig. 4.11, 4.12). We observe some signals of increased rising air over Northern India and East China by 2054 (Fig. 4.8-4.10), which calls for unstable atmospheric conditions and increased precipitation over these regions.

All models agree that the Indian Ocean will experience increased precipitation (Fig. 4.14, 4.15). This corresponds to the vertical mass flux over the same area, indicating instability (Fig. 4.8-4.10). While this change may be attributed to mitigated BC emissions, it is essential to note that fSSTs also play a role, and the models do not factor in the dynamic interplay between the ocean and atmosphere.

5.4 The Influences of Reducing BC Emissions on the Asian Summer Monsoon

Numerous studies have demonstrated the important role of aerosols in driving precipitation changes (e.g., Wu, P. et al. (2013), Menon et al. (2002); Wilcox et al. (2013)), as increased anthropogenic aerosols have been observed to contribute to the weakening of the ASM in the latter half of the 20th century (Bollasina et al., 2011; Polson et al., 2014; Song et al., 2014). Moreover, researchers have studied the impact of rapid reductions of anthropogenic aerosols on global and ASM precipitation. Wilcox et al. (2020) conducted one such study. The research

shows that strict air quality measures can increase global and ASM precipitation relative to historical observations from 1980-2014. This study also indicates that the influence of anthropogenic aerosols on precipitation patterns diminishes toward the end of the 21st century as GHGs become more dominant.

The current study differs in focusing solely on the climatic impacts of BC emissions, disregarding other aerosol species and GHGs. Previous studies have demonstrated how increased BC forcing can significantly influence the ASM, but their conclusions differ. Some studies have indicated weakening (e.g., Lau, K. M. et al. (2006), Lau, K.-M. and Kim (2006)), while other studies indicate increased precipitation due to BC (e.g., Chung and Ramanathan (2006), Ramanathan et al. (2005), Meehl et al. (2008)). Generally, the effects of increased BC on the ASM have been suggested to be inconsistent due to their strong dependency on differences in land or sea low-level thermal feedback (Xie et al., 2020).

The models and results of the current study also display inconsistency in response to reduced BC emissions. From the JJA-mean precipitation analysis in Figure 4.15, it can be observed that MIROC and MPI-ESM models generally reproduce enhanced responses to those associated with the ASM (see Fig. 4.1). These responses include the initiation of the monsoon over the central and southern parts of the Indochinese Peninsula, southwesterly winds bringing moisture from this area and the South China Sea to Southeast China. Northeast China will experience enhanced drought, and unstable atmospheric conditions over the Tibetan Plateau will also cause increased precipitation over this area. These results suggest that BC emissions may not be a significant driver of the ASM in these models, indicating that other forcing agents dominate. It should also be noted that only MIROC produces statistically significant results for precipitation out of these two models.

UKESM, on the other hand, projects significantly reduced precipitation levels over India, which is the opposite of what was initially expected. This is also despite the projection of surface warming (Fig. 4.7) and the resulting enhanced land-sea gradient. This discrepancy is, however, related to the slow response, which is not accurately represented with the use of fSSTs. Previous studies have also found that decreased carbonaceous aerosols and continued sulfate increases can weaken the South Asian monsoon over time, as this induces atmospheric

cooling (Das et al., 2020). We can also relate UKESM's response to a reduced semi-direct effect and altered convective activity, as explained in section 5.3.

UKESM also projects increased precipitation by the southern slope of the Tibetan Plateau, although the area is seemingly subject to stable atmospheric conditions (Fig. 4.8-4.10). This is primarily attributed to the unstable atmosphere above the Plateau. It has been proposed that increased amounts of absorbing aerosols near the surface of this area could enhance its “heat-pump” effect by intensifying convection and, thus, precipitation (Zhao et al., 2019). Reducing BC is, therefore, expected to reduce additional atmospheric heating, leading to less deep convection and precipitation and weakening the semi-direct effect. Nonetheless, the "heat pump" effect still dominates in the models' projections. Due to its elevation, the Tibetan Plateau heats up more during the day than the surrounding areas. It creates a low-pressure area as warm air rises and draws in humidity from the Indian Ocean (Ye & Wu, 1998). When lifted, the moist air cools and condenses to form clouds and precipitation.

Based on a recent study conducted by Xie et al. (2020), the ASM’s response to BC indicates a correlation between increased levels of BC and enhanced ASM precipitation due to increased upper-level atmospheric temperature over Asia. This suggests that lowering BC emissions would have a contrasting effect, though this was solely significantly observed in UKESM and not in MIROC and MPI-ESM.

As mentioned, the ASM activity is influenced by a range of factors, some of which are external and others internal. These include the Tibetan Plateau, SSTs, other atmospheric constituents, and atmospheric circulation variability. The variations among models projecting the monsoon's behavior are likely attributed to their ability or inability to factor in these mechanisms.

5.5 Comparison and Evaluation of Utilized ESMs

This section discusses the three ESMs utilized in this analysis, focusing on their suitability for projecting climate responses to reductions in BC emissions.

Using three different climate models to study the effects of reducing BC emissions provides unique insights into how each model interprets atmospheric processes and feedback mechanisms. Nevertheless, the approach presents challenges, such as diverse outcomes,

resource requirements for running simulations, and accurate interpretation of each model's output. Additionally, focusing specifically on BC emissions in each model may not capture the models' ability to interact with other atmospheric constituents, which limits the understanding of broader climate system responses. Therefore, utilizing three separate models is a valuable but complex approach to examining the individual and variable responses of the climate system to BC reduction.

The models utilized in this thesis exhibit both advantages and disadvantages when employed to study aerosols. UKESMs' high vertical layering allows for detailed atmospheric process simulation, especially in the upper atmosphere (Sellar et al., 2019). MIROC's higher resolution provides more complex spatial data for regional analysis and comprehensively represents atmospheric processes (Tatebe et al., 2019). MPI-ESM is suitable for studying the interactions between BC and climate. Nevertheless, its coarse resolution and limited number of vertical layers may hinder its ability to capture fine-scale regional variations (Mauritsen et al., 2019). UKESM delivers a comprehensive atmosphere analysis and generates the most robust outputs with distinct patterns of change. However, its precipitation responses are generally sensitive to convective activity. MIROC's higher spatial resolution for regional analysis appears to produce more intricate outputs at the regional level but contains more random noise. Still, it is less sensitive to BC changes than the two other models. Lastly, MPI-ESM provides somewhat vague and noisy outputs, and trends are more challenging to identify. Examples that capture these differences in model characteristics are Figure 4.14, where regional-mean annual-mean precipitation anomalies are simulated, and Figure 4.8, where regional-mean annual-mean vertical mass flux anomalies are simulated.

fSST simulations help identify rapid adjustments to aerosol concentrations, such as fast changes in atmospheric heating profiles and lapse rates, alterations in relative humidity profiles, and shifts in cloud and precipitation patterns. However, they are not ideal for surface temperature adjustments, and precipitation responses over the oceans exhibit quite noisy patterns. Coupled system effects, on the other hand, can have an impact on clouds, circulation, monsoon patterns, and precipitation response, but on a much slower time scale dependent on surface temperature and with more apparent and evident responses (Wilcox et al., 2023). Therefore, fSST simulations are preferred to observe response patterns from rapid adjustments and are utilized in this study.

5.6 Limitations and Uncertainties

When delivering a thesis on the intricate subject of aerosols, it is essential to acknowledge that the narrative presented needs to be more encompassing and has limitations. This selectiveness has resulted in notable uncertainties.

Determining the exact impact of BC is a multifaceted process that demands meticulous analysis of numerous factors to ensure that climate models can accurately isolate BC's influence. This involves utilizing precise measurement techniques to account for BC's spatial and temporal variability and observing how changes in atmospheric conditions affect the particle's optical properties. Current global climate models may also underestimate or overestimate the surface BC mass and BC absorption efficiency and how temperature changes are distributed vertically due to the oversimplification of complex BC microphysical and mixing properties (Chen et al., 2023; Xie et al., 2020), and thus may provide inconsistent responses. Global average absorption by BC remains challenging for climate models to estimate (Samset, B. H. et al., 2018). Consequently, the true impact of reducing BC cannot be determined with a high degree of accuracy.

Another challenge is identifying the mechanisms that cause the observed changes, particularly as BC is involved in various climatic interactions. To simplify the analysis, we concentrate only on direct and semi-direct effects and disregard indirect effects and BC deposition.

The Tibetan Plateau, a region important for the Asian monsoon dynamics, presents specific uncertainties in this analysis. UKESM and MIROC provide limited data for this area, while MPI-ESM generates noisy or inconsistent patterns, complicating interpretation. Moreover, excluding pre- and post-monsoon seasons from the seasonal analysis limits our understanding of the scope of the ASM response. Additionally, the study does not consider seasonal-mean vertical air temperature due to time constraints, which could provide additional insights into the response during the summer monsoon season.

The study is limited to a single future scenario, SSP3-7.0, often considered a worst-case scenario. While this approach helps magnify changes for easier identification, it may also exaggerate realistic changes. Moreover, the analysis does not account for aerosol composition changes (SSA) or other atmospheric components (other aerosols, GHGs) and how they affect the atmospheric heating rate.

This thesis's significant challenge is the uncertainty resulting from the models' limitations, especially in projecting the ASM. Relying on only three climate models, each with just one run has resulted in arbitrary patterns arising from internal variability, hindering accurate monsoon projections. The monsoon is already influenced by a complex interplay of thermodynamic and dynamic mechanisms that vary significantly across different models (Monerie et al., 2021). Enhancing the robustness of these projections would require incorporating additional models with a higher average of ensemble members, which would mitigate this uncertainty (Deser et al., 2020). However, this approach was not feasible due to time constraints. Lastly, the limited data availability for MIROC and MPI-ESM, extending only to 2054, restricts the ability to validate climatic patterns as effectively as with UKESM.

5.7 Recommendations for Future Research

In the context of climate research, South and East Asia hold particular importance due to their status as significant aerosol and precursor sources and the profound influence of the Asian monsoon. Therefore, further exploration into the climate responses to reductions in BC emissions in Asia is essential. Such studies are crucial to understanding the complex mechanisms underlying these responses and assessing whether mitigating BC emissions in Asia poses a climate risk, which is still uncertain.

To advance our understanding of the climatic effects of BC forcing in climate modeling, it is essential to prioritize research that reduces associated uncertainties. This can be achieved by improving measurement and observational techniques for aerosols, minimizing the uncertainty in AAOD retrieval. To achieve accuracy in estimations, it is recommended that a range of realistic perturbations of BC emissions be evaluated rather than restricting the focus solely to extreme scenarios. Additionally, it is advisable to include the analysis of aerosol surface deposition and ACI to comprehensively understand the relevant factors contributing to the phenomenon under examination. A multi-model ensemble approach should also be

used to reduce uncertainties surrounding internal variability and the complex internal and external mechanisms that influence the ASM, ultimately leading to a more precise understanding of potential climate impacts.

Efforts focused on deepening our comprehension of BC's role in the climate system, particularly in the climatically intricate regions of South and East Asia, will have the potential to contribute to more effective climate policies and strategies.

6 Conclusions

This thesis delves into the responses from a future phaseout of global BC emissions on different climate variables, with precipitation responses as the primary focus. The analysis examines the anomalies between the SSP3-7.0 and SSP3-7.0 low BC scenarios with three distinct ESMs in fixed-SST mode for 2015-2034 and 2035-2054 (up to 2094 for UKESM). Furthermore, the study highlights the most significant climate responses in South and East Asia and establishes possible correlations with the Asian Summer Monsoon (ASM).

The results reveal that a rapid reduction in BC emissions significantly reduces regional mean AAOD and generally reduces tropospheric heating rates for all models. Nonetheless, regional mean and seasonal mean surface temperature, vertical mass flux, and precipitation responses vary depending on the model employed.

Our observations indicate that MIROC and MPI-ESM projects enhanced responses similar to those associated with the ASM by 2054. This suggests that the role of BC-induced shortwave absorption in driving ASM weather patterns may not be significant for these models and that other factors may be the primary contributors. However, this study could not include the effects of sea-surface temperature change, which could affect this conclusion. Interestingly, UKESM projects significant reductions in precipitation over India by 2054, which can be linked to reduced convective activity and semi-direct effects due to the atmospheric cooling associated with BC removal.

The findings of UKESM for India suggest a potentially unforeseen climate impact of reducing BC emissions. The absence of BC in the atmosphere could lead to surface warming and tropospheric cooling, stimulating a turbulent vertical mass flux at 850 hPa. However, there is less convective activity at 250 hPa, resulting in less precipitation. Therefore, additional investigations incorporating these effects with ASM circulation mechanisms are necessary to provide a more comprehensive understanding of this phenomenon.

In conclusion, this thesis offers valuable insights into possible climatic responses arising from a future rapid phaseout of BC emissions across South and East Asia. Nevertheless, the variations observed between the models employed in this experiment emphasize the necessity for additional research into monsoon mechanisms regarding BC and adopting a multi-model ensemble approach to minimize the effects of internal variability.

REFERENCES

Acosta Navarro, J. C., Ekman, A. M. L., Pausata, F. S. R., Lewinschal, A., Varma, V., Seland, Ø., . . . Hansson, H. C. (2017). Future Response of Temperature and Precipitation to Reduced Aerosol Emissions as Compared with Increased Greenhouse Gas Concentrations. *Journal of Climate, 30*(3), 939-954. doi: https://doi.org/10.1175/JCLI-D-16-0466.1

Allen, M. R., & Ingram, W. J. (2002). Constraints on future changes in climate and the hydrologic cycle. *Nature, 419*(6903), 224-232. doi: https://doi.org/10.1038/nature01092

Almethen, O., & Aldaithan, Z. (2017). The State of Atmosphere Stability and Instability Effects on Air Quality. *The International Journal of Engineering and Science, 06*, 74-79. doi: https://doi.org/10.9790/1813-0604017479

Andreae, M. O., & Crutzen, P. J. (1997). Atmospheric Aerosols: Biogeochemical Sources and Role in Atmospheric Chemistry. *Science, 276*(5315), 1052-1058. doi: https://doi.org/10.1126/science.276.5315.1052

Andreae, M. O., & Gelencsér, A. (2006). Black carbon or brown carbon? The nature of light-absorbing carbonaceous aerosols. *Atmos. Chem. Phys., 6*(10), 3131-3148. doi: https://doi.org/10.5194/acp-6-3131-2006

Andrews, T., Forster, P. M., Boucher, O., Bellouin, N., & Jones, A. (2010). Precipitation, radiative forcing and global temperature change. *Geophysical Research Letters, 37*(14). doi: https://doi.org/10.1029/2010GL043991

Ansari, K., & Ramachandran, S. (2023). Radiative effects of absorbing aerosol types over South Asia. *Science of The Total Environment, 858*, 159969. doi: https://doi.org/10.1016/j.scitotenv.2022.159969

Baede, A. P. M., Ahlonsou, E., Ding, Y., & Schimel, D. (2001). The Climate System: an Overview. In *Climate Change 2001: The Scientific Basis. Contribution of Working Group I to the Third Assessment Report of the Intergovernmental Panel on Climate Change.* (pp. 87-98). Cambridge University Press, Cambridge, United Kingdom and New York, NY, USA: IPCC. doi.

Bala, G., Caldeira, K., & Nemani, R. (2010). Fast versus slow response in climate change: implications for the global hydrological cycle. *Climate Dynamics, 35*(2), 423-434. doi: https://doi.org/10.1007/s00382-009-0583-y

Beck, H. E., Zimmermann, N. E., McVicar, T. R., Vergopolan, N., Berg, A., & Wood, E. F. (2018). Present and future Köppen-Geiger climate classification maps at 1-km resolution. *Scientific Data, 5*(1), 180214. doi: https://doi.org/10.1038/sdata.2018.214

Bellouin, N., Quaas, J., Morcrette, J. J., & Boucher, O. (2013). Estimates of aerosol radiative forcing from the MACC re-analysis. *Atmos. Chem. Phys., 13*(4), 2045-2062. doi: https://doi.org/10.5194/acp-13-2045-2013

Bergstrom, R. W., Pilewskie, P., Russell, P. B., Redemann, J., Bond, T. C., Quinn, P. K., & Sierau, B. (2007). Spectral absorption properties of atmospheric aerosols. *Atmos. Chem. Phys., 7*(23), 5937-5943. doi: https://doi.org/10.5194/acp-7-5937-2007

Bollasina, M. A., Ming, Y., & Ramaswamy, V. (2011). Anthropogenic Aerosols and the Weakening of the South Asian Summer Monsoon. *Science, 334*(6055), 502-505. doi: https://doi.org/10.1126/science.1204994

Bollasina, M. A., Ming, Y., Ramaswamy, V., Schwarzkopf, M. D., & Naik, V. (2014). Contribution of local and remote anthropogenic aerosols to the twentieth century weakening of the South Asian Monsoon. *Geophysical Research Letters, 41*(2), 680-687. doi: https://doi.org/10.1002/2013GL058183

Bond, T. C., Doherty, S. J., Fahey, D. W., Forster, P. M., Berntsen, T., DeAngelo, B. J., . . . Zender, C. S. (2013). Bounding the role of black carbon in the climate system: A scientific assessment. *Journal of Geophysical Research: Atmospheres, 118*(11), 5380-5552. doi: https://doi.org/10.1002/jgrd.50171

Bordoni, S., & Schneider, T. (2008). Monsoons as eddy-mediated regime transitions of the tropical overturning circulation. *Nature Geoscience, 1*(8), 515-519. doi: https://doi.org/10.1038/ngeo248

Boucher, O. (2015a). Atmospheric Aerosols. In *Atmospheric Aerosols: Properties and Climate Impacts* O. Boucher, (pp. 9-24). Dordrecht: Springer Netherlands. doi: https://doi.org/10.1007/978-94-017-9649-1_2

Boucher, O. (2015b). General Introduction. In *Atmospheric Aerosols: Properties and Climate Impacts* (pp. 1-8). Dordrecht: Springer Netherlands. doi: https://doi.org/10.1007/978-94-017-9649-1_1

Boucher, O. (2015c). In Situ and Remote Sensing Measurements of Aerosols. In *Atmospheric Aerosols: Properties and Climate Impacts* (pp. 129-160). Dordrecht: Springer Netherlands. doi: https://doi.org/10.1007/978-94-017-9649-1_6

Brown, P. T., Li, W., Li, L., & Ming, Y. (2014). Top-of-atmosphere radiative contribution to unforced decadal global temperature variability in climate models. *Geophysical Research Letters, 41*(14), 5175-5183. doi: https://doi.org/10.1002/2014GL060625

Byrne, M. P., Pendergrass, A. G., Rapp, A. D., & Wodzicki, K. R. (2018). Response of the Intertropical Convergence Zone to Climate Change: Location, Width, and Strength. *Current Climate Change Reports, 4*(4), 355-370. doi: https://doi.org/10.1007/s40641-018-0110-5

Carslaw, K. S. (2022a). Aerosol in the climate system. In *Aerosols and Climate* K. S. Carslaw, (pp. 9-52): Elsevier. doi: https://doi.org/10.1016/B978-0-12-819766-0.00008-0

Carslaw, K. S. (2022b). Chapter 5 - Aerosol processes. In *Aerosols and Climate* K. S. Carslaw, (pp. 135-185): Elsevier. doi: https://doi.org/10.1016/B978-0-12-819766-0.00007-9

Carslaw, K. S., & Pringle, K. (2022). Chapter 4 - Global aerosol properties. In *Aerosols and Climate* K. S. Carslaw, (pp. 101-133): Elsevier. doi: https://doi.org/10.1016/B978-0-12-819766-0.00011-0

Chahine, M. T. (1992). The hydrological cycle and its influence on climate. *Nature, 359*(6394), 373-380. doi: https://doi.org/10.1038/359373a0

Chen, G., Wang, J., Wang, Y., Wang, J., Jin, Y., Cheng, Y., . . . Liu, C. (2023). An Aerosol Optical Module With Observation-Constrained Black Carbon Properties for Global Climate Models. *Journal of Advances in Modeling Earth Systems, 15*(10), e2022MS003501. doi: https://doi.org/10.1029/2022MS003501

Cheng, H., Edwards, R. L., Sinha, A., Spötl, C., Yi, L., Chen, S., . . . Zhang, H. (2016). The Asian monsoon over the past 640,000 years and ice age terminations. *Nature, 534*(7609), 640-646. doi: https://doi.org/10.1038/nature18591

Chung, C. E., & Ramanathan, V. (2006). Weakening of North Indian SST Gradients and the Monsoon Rainfall in India and the Sahel. *Journal of Climate, 19*(10), 2036-2045. doi: https://doi.org/10.1175/JCLI3820.1

Collins, W. D. (2019). *Revealing the Radiative Forcing by Well-Mixed Greenhouse Gases: From Derivation and Detection to Future Discoveries*. https://ui.adsabs.harvard.edu/abs/2019AGUFMGC34E..01C

Collins, W. J., Lamarque, J. F., Schulz, M., Boucher, O., Eyring, V., Hegglin, M. I., . . . Smith, S. J. (2017). AerChemMIP: quantifying the effects of chemistry and aerosols in CMIP6. *Geosci. Model Dev., 10*(2), 585-607. doi: https://doi.org/10.5194/gmd-10-585-2017

Das, S., Giorgi, F., Giuliani, G., Dey, S., & Coppola, E. (2020). Near-Future Anthropogenic Aerosol Emission Scenarios and Their Direct Radiative Effects on the Present-Day Characteristics of the Indian Summer Monsoon. *Journal of Geophysical Research: Atmospheres, 125*(4), e2019JD031414. doi: https://doi.org/10.1029/2019JD031414

Deser, C., Lehner, F., Rodgers, K. B., Ault, T., Delworth, T. L., DiNezio, P. N., . . . Ting, M. (2020). Insights from Earth system model initial-condition large ensembles and future prospects. *Nature Climate Change, 10*(4), 277-286. doi: https://doi.org/10.1038/s41558-020-0731-2

Ding, A. J., Huang, X., Nie, W., Sun, J. N., Kerminen, V.-M., Petäjä, T., . . . Fu, C. B. (2016). Enhanced haze pollution by black carbon in megacities in China. *Geophysical Research Letters, 43*(6), 2873-2879. doi: https://doi.org/10.1002/2016GL067745

Eyring, V., Bony, S., Meehl, G. A., Senior, C. A., Stevens, B., Stouffer, R. J., & Taylor, K. E. (2016). Overview of the Coupled Model Intercomparison Project Phase 6 (CMIP6) experimental design and organization. *Geosci. Model Dev., 9*(5), 1937-1958. doi: https://doi.org/10.5194/gmd-9-1937-2016

Forster, P., Storelvmo, T., Armour, K., Collins, W., Dufresne, J.-L., Frame, D., . . . H., Z. (2021). The Earth's Energy Budget, Climate Feedbacks, and Climate Sensitivity. In *Climate Change 2021: The Physical Science Basis. Contribution of Working Group I to the Sixth Assessment Report of the Intergovernmental Panel on Climate Change* V. [Masson-Delmotte, P. Zhai, A. Pirani, S.L. Connors, C. Péan, S. Berger, N. Caud, Y. Chen, L. Goldfarb, M.I. Gomis, M. Huang, K. Leitzell, E. Lonnoy, J.B.R. Matthews, T.K. Maycock, T. Waterfield, O. Yelekçi, R. Yu, and B. Zhou (eds.)]. (pp. 923–1054). Cambridge University Press, Cambridge, United Kingdom and New York, NY, USA: IPCC. doi: https://doi.org/10.1017/9781009157896.009.

Forster, P. M., Richardson, T., Maycock, A. C., Smith, C. J., Samset, B. H., Myhre, G., . . . Schulz, M. (2016). Recommendations for diagnosing effective radiative forcing from climate models for CMIP6. *Journal of Geophysical Research: Atmospheres, 121*(20), 12,460-412,475. doi: https://doi.org/10.1002/2016JD025320

Fowler, D., Brimblecombe, P., Burrows, J., Heal, M. R., Grennfelt, P., Stevenson, D. S., . . . Vieno, M. (2020). A chronology of global air quality. *Philosophical Transactions of the Royal Society A: Mathematical, Physical and Engineering Sciences, 378*(2183), 20190314. doi: https://doi.org/10.1098/rsta.2019.0314

Fujimori, S., Hasegawa, T., Masui, T., Takahashi, K., Herran, D. S., Dai, H., . . . Kainuma, M. (2017). SSP3: AIM implementation of Shared Socioeconomic Pathways. *Global Environmental Change, 42*, 268-283. doi: https://doi.org/10.1016/j.gloenvcha.2016.06.009

Ganopolski, A. (2019). Climate Change Models. In *Encyclopedia of Ecology (Second Edition)* B. Fath, (pp. 48-57). Oxford: Elsevier. doi: https://doi.org/10.1016/B978-0-12-409548-9.11166-2

Giles, D. M., Holben, B. N., Eck, T. F., Sinyuk, A., Smirnov, A., Slutsker, I., . . . Schafer, J. S. (2012). An analysis of AERONET aerosol absorption properties and classifications representative of aerosol source regions. *Journal of Geophysical Research: Atmospheres, 117*(D17). doi: https://doi.org/10.1029/2012JD018127

Guilyardi, E., Balaji, V., Lawrence, B., Callaghan, S., Deluca, C., Denvil, S., . . . Taylor, K. (2013). Documenting Climate Models and Their Simulations. *Bull. Amer. Met. Soc., 94*, 623-627. doi: https://doi.org/10.1175/BAMS-D-11-00035.1

Haywood, J. M., & Ramaswamy, V. (1998). Global sensitivity studies of the direct radiative forcing due to anthropogenic sulfate and black carbon aerosols. *Journal of Geophysical Research: Atmospheres, 103*(D6), 6043-6058. doi: https://doi.org/10.1029/97JD03426

Herbert, R., Wilcox, L. J., Joshi, M., Highwood, E., & Frame, D. (2022). Nonlinear response of Asian summer monsoon precipitation to emission reductions in South and East Asia. *Environmental Research Letters, 17*(1), 014005. doi: https://doi.org/10.1088/1748-9326/ac3b19

Herbertson, A. J. (1901). Outlines of Physiography An Introduction to the Study of the Earth. *Nature, 64*(1657), p. 118. doi: https://doi.org/10.1038/064325b0

Holben, B. N., Eck, T. F., Slutsker, I., Tanré, D., Buis, J. P., Setzer, A., . . . Smirnov, A. (1998). AERONET—A Federated Instrument Network and Data Archive for Aerosol Characterization. *Remote Sensing of Environment, 66*(1), 1-16. doi: https://doi.org/10.1016/S0034-4257(98)00031-5

Holben, B. N., Tanré, D., Smirnov, A., Eck, T. F., Slutsker, I., Abuhassan, N., . . . Zibordi, G. (2001). An emerging ground-based aerosol climatology: Aerosol optical depth from AERONET. *Journal of Geophysical Research: Atmospheres, 106*(D11), 12067-12097. doi: https://doi.org/10.1029/2001JD900014

IPCC. (2013). The Physical Science Basis. . In *Contribution of Working Group I to the Fifth Assessment Report of the Intergovernmental Panel on Climate Change* T. F. Stocker, D. Qin, G.-K. Plattner, M. Tignor, S.K. Allen, J. Boschung, A. Nauels, Y. Xia, V. Bex and P.M. Midgley (eds.), (pp. 1535). Cambridge University Press, Cambridge, United Kingdom and New York, NY, USA. doi. Retrieved from https://www.ipcc.ch/report/ar5/wg1/

IPCC. (2021). Climate Change 2021: The Physical Science Basis. Contribution of Working Group I to the Sixth Assessment Report of the Intergovernmental Panel on Climate Change. In V. [Masson-Delmotte, P. Zhai, A. Pirani, S.L. Connors, C. Péan, S. Berger, N. Caud, Y. Chen, L. Goldfarb, M.I. Gomis, M. Huang, K. Leitzell, E. Lonnoy, J.B.R. Matthews, T.K. Maycock, T. Waterfield, O. Yelekçi, R. Yu, and B. Zhou (eds.)], (pp. 2391). Cambridge University Press, Cambridge, United Kingdom and New York, NY, USA. doi: https://doi.org/10.1017/9781009157896

IPCC. (2023). Climate Change 2023: Synthesis Report. Contribution of Working Groups I, II and III to the Sixth Assessment Report of the Intergovernmental Panel on Climate Change. [Core Writing Team, H. Lee and J. Romero (eds.)]. Retrieved from https://www.ipcc.ch/report/ar6/syr/downloads/report/IPCC_AR6_SYR_FullVolume.pdf

Klimont, Z., Kupiainen, K., Heyes, C., Purohit, P., Cofala, J., Rafaj, P., . . . Schöpp, W. (2017). Global anthropogenic emissions of particulate matter including black carbon. *Atmos. Chem. Phys., 17*(14), 8681-8723. doi: https://doi.org/10.5194/acp-17-8681-2017

Kloster, S., Dentener, F., Feichter, J., Raes, F., Lohmann, U., Roeckner, E., & Fischer-Bruns, I. (2010). A GCM study of future climate response to aerosol pollution reductions. *Climate Dynamics, 34*(7), 1177-1194. doi: https://doi.org/10.1007/s00382-009-0573-0

Kokhanovsky, A. (2008). *Aerosol Optics: Light Absorption and Scattering by Particles in the Atmosphere*. doi: https://doi.org/10.1007/978-3-540-49909-1

Köppen, W. P. (1936). *Das geographische System der Klimate: Mit 14 Textfiguren*: Borntraeger. doi.

Lau, K.-M., & Kim, K.-M. (2006). Observational relationships between aerosol and Asian monsoon rainfall, and circulation. *Geophysical Research Letters, 33*(21). doi: https://doi.org/10.1029/2006GL027546

Lau, K. M., Kim, M. K., & Kim, K. M. (2006). Asian summer monsoon anomalies induced by aerosol direct forcing: the role of the Tibetan Plateau. *Climate Dynamics, 26*(7), 855-864. doi: https://doi.org/10.1007/s00382-006-0114-z

Lau, W. K. M. (2016). The aerosol-monsoon climate system of Asia: A new paradigm. *Journal of Meteorological Research, 30*(1), 1-11. doi: https://doi.org/10.1007/s13351-015-5999-1

Li, C., McLinden, C., Fioletov, V., Krotkov, N., Carn, S., Joiner, J., . . . Dickerson, R. R. (2017). India Is Overtaking China as the World's Largest Emitter of Anthropogenic Sulfur Dioxide. *Scientific Reports, 7*(1), 14304. doi: https://doi.org/10.1038/s41598-017-14639-8

Li, J., Carlson, B. E., Yung, Y. L., Lv, D. R., Hansen, J., Penner, J. E., . . . Dong, Y. M. (2022). Scattering and absorbing aerosols in the climate system. *Nature Reviews Earth & Environment, 3*(6), 363-379. doi: https://doi.org/10.1038/s43017-022-00296-7

Li, Z., Lau, W. K.-M., Ramanathan, V., Wu, G., Ding, Y., Manoj, M. G., . . . Brasseur, G. P. (2016). Aerosol and monsoon climate interactions over Asia. *Reviews of Geophysics, 54*(4), 866-929. doi: https://doi.org/10.1002/2015RG000500

Liao, H., & Seinfeld, J. H. (1998). Effect of clouds on direct aerosol radiative forcing of climate. *Journal of Geophysical Research: Atmospheres, 103*(D4), 3781-3788. doi: https://doi.org/10.1029/97JD03455

Liepert, B. G., & Previdi, M. (2009). Do Models and Observations Disagree on the Rainfall Response to Global Warming? *Journal of Climate, 22*(11), 3156-3166. doi: https://doi.org/10.1175/2008JCLI2472.1

Liu, D., He, C., Schwarz, J. P., & Wang, X. (2020). Lifecycle of light-absorbing carbonaceous aerosols in the atmosphere. *npj Climate and Atmospheric Science, 3*(1), 40. doi: https://doi.org/10.1038/s41612-020-00145-8

Liu, L., Shawki, D., Voulgarakis, A., Kasoar, M., Samset, B. H., Myhre, G., . . . Takemura, T. (2018). A PDRMIP Multimodel Study on the Impacts of Regional Aerosol Forcings on Global and Regional Precipitation. *Journal of Climate, 31*(11), 4429-4447. doi: https://doi.org/10.1175/JCLI-D-17-0439.1

Lund, M. T., Sahu, S. K., Mangaraj, P., Samset, B. H., Chowdhury, S., Myhre, G., & Johansen, A. N. (2023). *Quantifying effects of Indian aerosol emissions on regional aerosol abundances, energy balance, and health impacts, using a novel national emission inventory*. Paper presented at the EGU General Assembly 2023, Vienna, Austria.

Lund, M. T., Aamaas, B., Stjern, C. W., Klimont, Z., Berntsen, T. K., & Samset, B. H. (2020). A continued role of short-lived climate forcers under the Shared Socioeconomic Pathways. *Earth Syst. Dynam., 11*(4), 977-993. doi: https://doi.org/10.5194/esd-11-977-2020

Mann, G. W., Carslaw, K. S., Reddington, C. L., Pringle, K. J., Schulz, M., Asmi, A., . . . Henzing, J. S. (2014). Intercomparison and evaluation of global aerosol microphysical

properties among AeroCom models of a range of complexity. *Atmos. Chem. Phys., 14*(9), 4679-4713. doi: https://doi.org/10.5194/acp-14-4679-2014

Mauritsen, T., Bader, J., Becker, T., Behrens, J., Bittner, M., Brokopf, R., . . . Roeckner, E. (2019). Developments in the MPI-M Earth System Model version 1.2 (MPI-ESM1.2) and Its Response to Increasing CO2. *Journal of Advances in Modeling Earth Systems, 11*(4), 998-1038. doi: https://doi.org/10.1029/2018MS001400

Meehl, G. A., Arblaster, J. M., & Collins, W. D. (2008). Effects of Black Carbon Aerosols on the Indian Monsoon. *Journal of Climate, 21*(12), 2869-2882. doi: https://doi.org/10.1175/2007JCLI1777.1

Menon, S., Hansen, J., Nazarenko, L., & Luo, Y. (2002). Climate Effects of Black Carbon Aerosols in China and India. *Science, 297*(5590), 2250-2253. doi: https://doi.org/10.1126/science.1075159

Mikhailov, E. F., Vlasenko, S. S., Podgorny, I. A., Ramanathan, V., & Corrigan, C. E. (2006). Optical properties of soot–water drop agglomerates: An experimental study. *Journal of Geophysical Research: Atmospheres, 111*(D7). doi: https://doi.org/10.1029/2005JD006389

Millar, R. J., Fuglestvedt, J. S., Friedlingstein, P., Rogelj, J., Grubb, M. J., Matthews, H. D., . . . Allen, M. R. (2017). Emission budgets and pathways consistent with limiting warming to 1.5 °C. *Nature Geoscience, 10*(10), 741-747. doi: https://doi.org/10.1038/ngeo3031

Mishra, A. K., Koren, I., & Rudich, Y. (2015). Effect of aerosol vertical distribution on aerosol-radiation interaction: A theoretical prospect. *Heliyon, 1*(2), e00036. doi: https://doi.org/10.1016/j.heliyon.2015.e00036

Mohanakumar, K. (2008). Stratosphere troposphere interactions: An introduction. In. doi: https://doi.org/10.1007/978-1-4020-8217-7

Monerie, P.-A., I Robson, J., J Dunstone, N., & G Turner, A. (2021). Skilful seasonal predictions of global monsoon summer precipitation with DePreSys3. *Environmental Research Letters, 16*(10), 104035. doi: https://doi.org/10.1088/1748-9326/ac2a65

Moorthy, K. K., Satheesh, S., Babu, S., & Saha, A. (2005). Large latitudinal gradients and temporal heterogeneity in aerosol black carbon and its mass mixing ratio over southern and northern oceans during a transcontinental cruise experiment. *Geophysical Research Letters - GEOPHYS RES LETT, 321*. doi: https://doi.org/10.1029/2005GL023267

Mosley, S. (2014). Environmental History of Air Pollution and Protection. In *The Basic Environmental History* M. Agnoletti & S. Neri Serneri, (pp. 143-169). Cham: Springer International Publishing. doi: https://doi.org/10.1007/978-3-319-09180-8_5

Myhre, G., Myhre, C. E.L., Samset, B. H. & Storelvmo, T. . (2013). Aerosols and their Relation to Global Climate and Climate Sensitivity. *Nature Education Knowledge, 4*(5). doi.

National Geographic, S. (2023, October 19). Atmosphere. Retrieved from https://education.nationalgeographic.org/resource/atmosphere/

Neubauer, D., Ferrachat, S., Siegenthaler-Le Drian, C., Stoll, J., Folini, D. S., Tegen, I., . . . Lohmann, U. (2019). *HAMMOZ-Consortium MPI-ESM1.2-HAM model output prepared for CMIP6 CMIP historical*. Retrieved from: https://doi.org/10.22033/ESGF/CMIP6.5016

O'Neill, B. C., Tebaldi, C., van Vuuren, D. P., Eyring, V., Friedlingstein, P., Hurtt, G., . . . Sanderson, B. M. (2016). The Scenario Model Intercomparison Project (ScenarioMIP) for CMIP6. *Geosci. Model Dev., 9*(9), 3461-3482. doi: https://doi.org/10.5194/gmd-9-3461-2016

Palmer, M. D., & McNeall, D. J. (2014). Internal variability of Earth's energy budget simulated by CMIP5 climate models. *Environmental Research Letters, 9*(3), 034016. doi: https://doi.org/10.1088/1748-9326/9/3/034016

Peel, M. C., Finlayson, B. L., & McMahon, T. A. (2007). Updated world map of the Köppen-Geiger climate classification. *Hydrol. Earth Syst. Sci., 11*(5), 1633-1644. doi: https://doi.org/10.5194/hess-11-1633-2007

Pendergrass, A. G., & Hartmann, D. L. (2012). Global-mean precipitation and black carbon in AR4 simulations. *Geophysical Research Letters, 39*(1). doi: https://doi.org/10.1029/2011GL050067

Pendergrass, A. G., & Hartmann, D. L. (2014). The Atmospheric Energy Constraint on Global-Mean Precipitation Change. *Journal of Climate, 27*(2), 757-768. doi: https://doi.org/10.1175/JCLI-D-13-00163.1

Petzold, A., Ogren, J. A., Fiebig, M., Laj, P., Li, S. M., Baltensperger, U., . . . Zhang, X. Y. (2013). Recommendations for reporting "black carbon" measurements. *Atmos. Chem. Phys., 13*(16), 8365-8379. doi: https://doi.org/10.5194/acp-13-8365-2013

Polson, D., Bollasina, M., Hegerl, G. C., & Wilcox, L. J. (2014). Decreased monsoon precipitation in the Northern Hemisphere due to anthropogenic aerosols. *Geophysical Research Letters, 41*(16), 6023-6029. doi: https://doi.org/10.1002/2014GL060811

Ramachandran, S. (2018). Aerosols and Climate Change: Present Understanding, Challenges, and Future Outlook. In *Land-Atmospheric Research Applications in South and Southeast Asia* K. P. Vadrevu, T. Ohara, & C. Justice, (pp. 341-378). Cham: Springer International Publishing. doi: https://doi.org/10.1007/978-3-319-67474-2_17

Ramachandran, S., & Rupakheti, M. (2022). Trends in the types and absorption characteristics of ambient aerosols over the Indo-Gangetic Plain and North China Plain in last two decades. *Science of The Total Environment, 831*, 154867. doi: https://doi.org/10.1016/j.scitotenv.2022.154867

Ramachandran, S., Rupakheti, M., & Cherian, R. (2022). Insights into recent aerosol trends over Asia from observations and CMIP6 simulations. *Sci Total Environ, 807*(Pt 1), 150756. doi: https://doi.org/10.1016/j.scitotenv.2021.150756

Ramachandran, S., Rupakheti, M., & Lawrence, M. G. (2020). Aerosol-induced atmospheric heating rate decreases over South and East Asia as a result of changing content and

composition. *Scientific Reports, 10*(1), 20091. doi: https://doi.org/10.1038/s41598-020-76936-z

Ramanathan, V., & Carmichael, G. (2008). Global and regional climate changes due to black carbon. *Nature Geoscience, 1*(4), 221-227. doi: https://doi.org/10.1038/ngeo156

Ramanathan, V., Chung, C., Kim, D., Bettge, T., Buja, L., Kiehl, J. T., . . . Wild, M. (2005). Atmospheric brown clouds: Impacts on South Asian climate and hydrological cycle. *Proceedings of the National Academy of Sciences, 102*(15), 5326-5333. doi: https://doi.org/10.1073/pnas.0500656102

Ramanathan, V., Crutzen, P. J., Kiehl, J. T., & Rosenfeld, D. (2001). Aerosols, Climate, and the Hydrological Cycle. *Science, 294*(5549), 2119-2124. doi: https://doi.org/10.1126/science.1064034

Randall, D. A., Wood, R. A., Bony, S., Colman, R., Fichefet, T., Fyfe, J., . . . K.E., T. (2007). Cilmate Models and Their Evaluation. In *Climate Change 2007: The Physical Science Basis. Contribution of Working Group I to the Fourth Assessment Report of the Intergovernmental Panel on Climate Change.* S. [Solomon, D. Qin, M. Manning, Z. Chen, M. Marquis, K.B. Averyt, M.Tignor and H.L. Miller (eds.)]. Cambridge University Press, Cambridge, United Kingdom and New York, NY, USA.: IPCC. doi. Retrieved from https://www.ipcc.ch/report/ar4/wg1/climate-models-and-their-evaluation/

Rao, S., & Dey, S. (2020). Consistent signal of aerosol indirect and semi-direct effect on water clouds in the oceanic regions adjacent to the Indian subcontinent. *Atmospheric Research, 232*, 104677. doi: https://doi.org/10.1016/j.atmosres.2019.104677

Rao, S., Klimont, Z., Smith, S. J., Van Dingenen, R., Dentener, F., Bouwman, L., . . . Tavoni, M. (2017). Future air pollution in the Shared Socio-economic Pathways. *Global Environmental Change, 42*, 346-358. doi: https://doi.org/10.1016/j.gloenvcha.2016.05.012

Riahi, K., van Vuuren, D. P., Kriegler, E., Edmonds, J., O'Neill, B. C., Fujimori, S., . . . Tavoni, M. (2017). The Shared Socioeconomic Pathways and their energy, land use, and greenhouse gas emissions implications: An overview. *Global Environmental Change, 42*, 153-168. doi: https://doi.org/10.1016/j.gloenvcha.2016.05.009

Richardson, T. B., Forster, P. M., Andrews, T., Boucher, O., Faluvegi, G., Fläschner, D., . . . Voulgarakis, A. (2018). Drivers of Precipitation Change: An Energetic Understanding. *Journal of Climate, 31*(23), 9641-9657. doi: https://doi.org/10.1175/JCLI-D-17-0240.1

Rotstayn, L. D., Collier, M. A., Chrastansky, A., Jeffrey, S. J., & Luo, J. J. (2013). Projected effects of declining aerosols in RCP4.5: unmasking global warming? *Atmos. Chem. Phys., 13*(21), 10883-10905. doi: https://doi.org/10.5194/acp-13-10883-2013

Rönkkö, T., Saarikoski, S., Kuittinen, N., Karjalainen, P., Keskinen, H., Järvinen, A., . . . Timonen, H. (2023). Review of black carbon emission factors from different anthropogenic sources. *Environmental Research Letters, 18*(3), 033004. doi: https://doi.org/10.1088/1748-9326/acbb1b

Salzmann, M. (2016). Global warming without global mean precipitation increase? *Science Advances, 2*(6), e1501572. doi: https://doi.org/10.1126/sciadv.1501572

Samset, B., Sand, M., Smith, C., Bauer, S., Forster, P., Fuglestvedt, J., . . . Schleussner, C. (2018). Climate Impacts From a Removal of Anthropogenic Aerosol Emissions. *Geophysical Research Letters, 45*. doi: https://doi.org/10.1002/2017GL076079

Samset, B. H. (2016). Aerosols and Climate. doi:https://doi.org/10.1093/acrefore/9780190228620.013.13

Samset, B. H. (2022). Aerosol absorption has an underappreciated role in historical precipitation change. *Communications Earth & Environment, 3*(1), 242. doi: https://doi.org/10.1038/s43247-022-00576-6

Samset, B. H., Lund, M. T., Bollasina, M., Myhre, G., & Wilcox, L. (2019). Emerging Asian aerosol patterns. *Nature Geoscience, 12*(8), 582-584. doi: https://doi.org/10.1038/s41561-019-0424-5

Samset, B. H., Myhre, G., Forster, P. M., Hodnebrog, Ø., Andrews, T., Faluvegi, G., . . . Voulgarakis, A. (2016). Fast and slow precipitation responses to individual climate forcers: A PDRMIP multimodel study. *Geophysical Research Letters, 43*(6), 2782-2791. doi: https://doi.org/10.1002/2016GL068064

Samset, B. H., Stjern, C. W., Andrews, E., Kahn, R. A., Myhre, G., Schulz, M., & Schuster, G. L. (2018). Aerosol Absorption: Progress Towards Global and Regional Constraints. *Current Climate Change Reports, 4*(2), 65-83. doi: https://doi.org/10.1007/s40641-018-0091-4

Sand, M., Samset, B., Tsigaridis, K., Bauer, S., & Myhre, G. (2020). Black Carbon and Precipitation: An Energetics Perspective. *Journal of Geophysical Research: Atmospheres, 125*. doi: https://doi.org/10.1029/2019JD032239

Sand, M., Samset, B. H., Myhre, G., Gliß, J., Bauer, S. E., Bian, H., . . . Watson-Parris, D. (2021). Aerosol absorption in global models from AeroCom phase III. *Atmos. Chem. Phys., 21*(20), 15929-15947. doi: https://doi.org/10.5194/acp-21-15929-2021

Satheesh, S. K., & Ramanathan, V. (2000). Large differences in tropical aerosol forcing at the top of the atmosphere and Earth's surface. *Nature, 405*(6782), 60-63. doi: https://doi.org/10.1038/35011039

Sellar, A. A., Jones, C. G., Mulcahy, J. P., Tang, Y., Yool, A., Wiltshire, A., . . . Zerroukat, M. (2019). UKESM1: Description and Evaluation of the U.K. Earth System Model. *Journal of Advances in Modeling Earth Systems, 11*(12), 4513-4558. doi: https://doi.org/10.1029/2019MS001739

Shin, S. K., Tesche, M., Müller, D., & Noh, Y. (2019). Technical note: Absorption aerosol optical depth components from AERONET observations of mixed dust plumes. *Atmos. Meas. Tech., 12*(1), 607-618. doi: https://doi.org/10.5194/amt-12-607-2019

Shindell, D., Lamarque, J. F., Unger, N., Koch, D., Faluvegi, G., Bauer, S., . . . Teich, H. (2008). Climate forcing and air quality change due to regional emissions reductions by economic sector. *Atmos. Chem. Phys., 8*(23), 7101-7113. doi: https://doi.org/10.5194/acp-8-7101-2008

Song, F., Zhou, T., & Qian, Y. (2014). Responses of East Asian summer monsoon to natural and anthropogenic forcings in the 17 latest CMIP5 models. *Geophysical Research Letters, 41*(2), 596-603. doi: https://doi.org/10.1002/2013GL058705

Stevens, B., & Bony, S. (2013). Water in the atmosphere. *Physics Today, 66*(6), 29-34. doi: https://doi.org/10.1063/pt.3.2009

Stjern, C. W., Samset, B. H., Myhre, G., Forster, P. M., Hodnebrog, Ø., Andrews, T., . . . Voulgarakis, A. (2017). Rapid Adjustments Cause Weak Surface Temperature Response to Increased Black Carbon Concentrations. *Journal of Geophysical Research: Atmospheres, 122*(21), 11,462-411,481. doi: https://doi.org/10.1002/2017JD027326

Streets, D. G., Shindell, D. T., Lu, Z., & Faluvegi, G. (2013). Radiative forcing due to major aerosol emitting sectors in China and India. *Geophysical Research Letters, 40*(16), 4409-4414. doi: https://doi.org/10.1002/grl.50805

Takemura, T., & Suzuki, K. (2019). Weak global warming mitigation by reducing black carbon emissions. *Scientific Reports, 9*(1), 4419. doi: https://doi.org/10.1038/s41598-019-41181-6

Tang, Q. (2020). Global change hydrology: Terrestrial water cycle and global change. *Science China Earth Sciences, 63*(3), 459-462. doi: https://doi.org/10.1007/s11430-019-9559-9

Tatebe, H., Ogura, T., Nitta, T., Komuro, Y., Ogochi, K., Takemura, T., . . . Kimoto, M. (2019). Description and basic evaluation of simulated mean state, internal variability, and climate sensitivity in MIROC6. *Geosci. Model Dev., 12*(7), 2727-2765. doi: https://doi.org/10.5194/gmd-12-2727-2019

Thorsen, T. J., Ferrare, R. A., Kato, S., & Winker, D. M. (2020). Aerosol Direct Radiative Effect Sensitivity Analysis. *Journal of Climate, 33*(14), 6119-6139. doi: https://doi.org/10.1175/JCLI-D-19-0669.1

Trenberth, K. E. (2018). Climate change caused by human activities is happening and it already has major consequences. *Journal of Energy & Natural Resources Law, 36*(4), 463-481. doi: https://doi.org/10.1080/02646811.2018.1450895

Twomey, S. (1977). The Influence of Pollution on the Shortwave Albedo of Clouds. *Journal of Atmospheric Sciences, 34*(7), 1149-1152. doi: https://doi.org/10.1175/1520-0469(1977)034<1149:TIOPOT>2.0.CO;2

UNCCS. (2019). *Climate action and support trends*. Retrieved from https://unfccc.int/sites/default/files/resource/Climate_Action_Support_Trends_2019.pdf

Undorf, S., Polson, D., Bollasina, M. A., Ming, Y., Schurer, A., & Hegerl, G. C. (2018). Detectable Impact of Local and Remote Anthropogenic Aerosols on the 20th Century

Changes of West African and South Asian Monsoon Precipitation. *Journal of Geophysical Research: Atmospheres, 123*(10), 4871-4889. doi: https://doi.org/10.1029/2017JD027711

Wang, B., & Ding, Q. (2008). Global monsoon: Dominant mode of annual variation in the tropics. *Dynamics of Atmospheres and Oceans, 44*(3), 165-183. doi: https://doi.org/10.1016/j.dynatmoce.2007.05.002

Westervelt, D. M., Horowitz, L. W., Naik, V., Golaz, J. C., & Mauzerall, D. L. (2015). Radiative forcing and climate response to projected 21st century aerosol decreases. *Atmos. Chem. Phys., 15*(22), 12681-12703. doi: https://doi.org/10.5194/acp-15-12681-2015

Wilcox, L. J., Allen, R. J., Samset, B. H., Bollasina, M. A., Griffiths, P. T., Keeble, J., . . . Westervelt, D. M. (2023). The Regional Aerosol Model Intercomparison Project (RAMIP). *Geosci. Model Dev., 16*(15), 4451-4479. doi: https://doi.org/10.5194/gmd-16-4451-2023

Wilcox, L. J., Highwood, E. J., & Dunstone, N. J. (2013). The influence of anthropogenic aerosol on multi-decadal variations of historical global climate. *Environmental Research Letters, 8*(2), 024033. doi: https://doi.org/10.1088/1748-9326/8/2/024033

Wilcox, L. J., Liu, Z., Samset, B. H., Hawkins, E., Lund, M. T., Nordling, K., . . . Turner, A. G. (2020). Accelerated increases in global and Asian summer monsoon precipitation from future aerosol reductions. *Atmos. Chem. Phys., 20*(20), 11955-11977. doi: https://doi.org/10.5194/acp-20-11955-2020

Wu, G., Liu, Y., He, B., Bao, Q., Duan, A., & Jin, F.-F. (2012). Thermal Controls on the Asian Summer Monsoon. *Scientific Reports, 2*(1), 404. doi: https://doi.org/10.1038/srep00404

Wu, P., Christidis, N., & Stott, P. (2013). Anthropogenic impact on Earth's hydrological cycle. *Nature Climate Change, 3*(9), 807-810. doi: https://doi.org/10.1038/nclimate1932

Xie, X., Myhre, G., Liu, X., Li, X., Shi, Z., Wang, H., . . . Liu, Y. (2020). Distinct responses of Asian summer monsoon to black carbon aerosols and greenhouse gases. *Atmos. Chem. Phys., 20*(20), 11823-11839. doi: https://doi.org/10.5194/acp-20-11823-2020

Yanai, M., & Wu, G.-X. (2006). Effects of the Tibetan Plateau. In *The Asian Monsoon* (pp. 513-549). Berlin, Heidelberg: Springer Berlin Heidelberg. doi: https://doi.org/10.1007/3-540-37722-0_13

Ye, D.-Z., & Wu, G.-X. (1998). The role of the heat source of the Tibetan Plateau in the general circulation. *Meteorology and Atmospheric Physics, 67*(1), 181-198. doi: https://doi.org/10.1007/BF01277509

Yoro, K. O., & Daramola, M. O. (2020). Chapter 1 - CO2 emission sources, greenhouse gases, and the global warming effect. In *Advances in Carbon Capture Eds:* M. R. Rahimpour, M. Farsi, & M. A. Makarem, (pp. 3-28): Woodhead Publishing. doi: https://doi.org/10.1016/B978-0-12-819657-1.00001-3

Zelinka, M. D., Myers, T. A., McCoy, D. T., Po-Chedley, S., Caldwell, P. M., Ceppi, P., . . . Taylor, K. E. (2020). Causes of Higher Climate Sensitivity in CMIP6 Models. *Geophysical Research Letters, 47*(1), e2019GL085782. doi: https://doi.org/10.1029/2019GL085782

Zhang, B. W. (2020). The Effect of Aerosols to Climate Change and Society. *Journal of Geoscience and Environment Protection, 8*, 55-78. doi: https://doi.org/10.4236/gep.2020.88006

Zhao, C., Yang, Y., Fan, H., Huang, J., Fu, Y., Zhang, X., . . . Menenti, M. (2019). Aerosol characteristics and impacts on weather and climate over the Tibetan Plateau. *National Science Review, 7*(3), 492-495. doi: https://doi.org/10.1093/nsr/nwz184

APPENDIX A

Software

Table A.1: Python modules utilized for data simulation and visualization.

Module Name	Version	Purpose of use
cartopy	0.22.0	Used for mapping, geographic projections, and plotting spatial data
cftime	1.6.2	Handling time formats used in climate data
datetime	3.11.1	Managing and manipulating dates and times
matplotlib	3.8.0	Plotting and visualizing data
numpy	1.24.4	Array and numerical processing
pandas	1.5.3	Data analysis and manipulation
scipy.stats	1.10.1	Statistical analysis, Students t-test
xarray	2023.8.0	Handling multi-dimensional arrays and datasets
zarr	2.16.1	Handling large, compressed, n-dimensional arrays

Hardware

The simulations were performed on resources provided by Sigma2 - the National Infrastructure for High Performance Computing and Data Storage in Norway. [3]

Table A.2: NIRD Technical Specifications.

Cluster	NIRD DL
Storage media	NL-SAS
Performance	66 GB/s
Capacity	25 PB
Interconnect	Balanced 200 Gbit/s
Protocol nodes	5 x 50 Gbit/s

[3] More information regarding NIRD and Sigma2 can be found here: https://documentation.sigma2.no/files_storage/nird_lmd.html

Norges miljø- og biovitenskapelige universitet
Noregs miljø- og biovitskapelege universitet
Norwegian University of Life Sciences

Postboks 5003
NO-1432 Ås
Norway